NATIONAL ADVISORY COMMITTEE FOR AERONAUTICS

REPORT No. 640

THE AERODYNAMIC CHARACTERISTICS OF FULL-SCALE PROPELLERS HAVING 2, 3, AND 4 BLADES OF CLARK Y AND R. A. F. 6 AIRFOIL SECTIONS

By EDWIN P. HARTMAN and DAVID BIERMANN

1938

AERONAUTIC SYMBOLS

1. FUNDAMENTAL AND DERIVED UNITS

	Symbol	Metric		English	
		Unit	Abbreviation	Unit	Abbreviation
Length	l	meter	m	foot (or mile)	ft. (or mi.)
Time	t	second	s	second (or hour)	sec. (or hr.)
Force	F	weight of 1 kilogram	kg	weight of 1 pound	lb.
Power	P	horsepower (metric)		horsepower	hp.
Speed	V	kilometers per hour	k.p.h.	miles per hour	m.p.h.
		meters per second	m.p.s.	feet per second	f.p.s.

2. GENERAL SYMBOLS

W, Weight$=mg$

g, Standard acceleration of gravity$=9.80665$ m/s^2 or 32.1740 ft./sec.^{2}

m, Mass$=\frac{W}{g}$

I, Moment of inertia$=mk^2$. (Indicate axis of radius of gyration k by proper subscript.)

μ, Coefficient of viscosity

ν, Kinematic viscosity

ρ, Density (mass per unit volume)

Standard density of dry air, 0.12497 kg-m^{-4}-s^2 at 15° C. and 760 mm; or 0.002378 lb.-ft.$^{-4}$ sec.^{2}

Specific weight of "standard" air, 1.2255 kg/m^3 or 0.07651 lb./cu. ft.

3. AERODYNAMIC SYMBOLS

S, Area

S_w, Area of wing

G, Gap

b, Span

c, Chord

$\frac{b^2}{S}$, Aspect ratio

V, True air speed

q, Dynamic pressure$=\frac{1}{2}\rho V^2$

L, Lift, absolute coefficient $C_L=\frac{L}{qS}$

D, Drag, absolute coefficient $C_D=\frac{D}{qS}$

D_0, Profile drag, absolute coefficient $C_{D_0}=\frac{D_0}{qS}$

D_i, Induced drag, absolute coefficient $C_{D_i}=\frac{D_i}{qS}$

D_p, Parasite drag, absolute coefficient $C_{D_p}=\frac{D_p}{qS}$

C, Cross-wind force, absolute coefficient $C_C=\frac{C}{qS}$

R, Resultant force

i_w, Angle of setting of wings (relative to thrust line)

i_t, Angle of stabilizer setting (relative to thrust line)

Q, Resultant moment

Ω, Resultant angular velocity

$\rho\frac{Vl}{\mu}$, Reynolds Number, where l is a linear dimension (e.g., for a model airfoil 3 in. chord, 100 m.p.h. normal pressure at 15° C., the corresponding number is 234,000; or for a model of 10 cm chord, 40 m.p.s., the corresponding number is 274,000)

C_p, Center-of-pressure coefficient (ratio of distance of c.p. from leading edge to chord length)

α, Angle of attack

ϵ, Angle of downwash

α_0, Angle of attack, infinite aspect ratio

α_i, Angle of attack, induced

α_a, Angle of attack, absolute (measured from zero-lift position)

γ, Flight-path angle

REPORT No. 640

THE AERODYNAMIC CHARACTERISTICS OF FULL-SCALE PROPELLERS HAVING 2, 3, AND 4 BLADES OF CLARK Y AND R. A. F. 6 AIRFOIL SECTIONS

By EDWIN P. HARTMAN and DAVID BIERMANN
Langley Memorial Aeronautical Laboratory

I-a

80779—38——1

NATIONAL ADVISORY COMMITTEE FOR AERONAUTICS

HEADQUARTERS, NAVY BUILDING, WASHINGTON, D. C.

LABORATORIES, LANGLEY FIELD, VA.

Created by act of Congress approved March 3, 1915, for the supervision and direction of the scientific study of the problems of flight (U. S. Code, Title 50, Sec. 151). Its membership was increased to 15 by act approved March 2, 1929. The members are appointed by the President, and serve as such without compensation.

TECHNICAL COMMITTEES

AERODYNAMICS
POWER PLANTS FOR AIRCRAFT
AIRCRAFT MATERIALS
AIRCRAFT STRUCTURES
AIRCRAFT ACCIDENTS
INVENTIONS AND DESIGNS

Coordination of Research Needs of Military and Civil Aviation

Preparation of Research Programs

Allocation of Problems

Prevention of Duplication

Consideration of Inventions

LANGLEY MEMORIAL AERONAUTICAL LABORATORY

LANGLEY FIELD, VA.

Unified conduct, for all agencies, of scientific research on the fundamental problems of flight.

OFFICE OF AERONAUTICAL INTELLIGENCE

WASHINGTON, D. C.

Collection, classification, compilation, and dissemination of scientific and technical information on aeronautics.

REPORT No. 640

THE AERODYNAMIC CHARACTERISTICS OF FULL-SCALE PROPELLERS HAVING 2, 3, AND 4 BLADES OF CLARK Y AND R. A. F. 6 AIRFOIL SECTIONS

By Edwin P. Hartman and David Biermann

SUMMARY

Aerodynamic tests were made of seven full-scale 10-foot-diameter propellers of recent design comprising three groups. The first group was composed of three propellers having Clark Y airfoil sections and the second group was composed of three propellers having R. A. F. 6 airfoil sections, the propellers of each group having 2, 3, and 4 blades. The third group was composed of two propellers, the 2-blade propeller taken from the second group and another propeller having the same airfoil section and number of blades but with the width and thickness 50 percent greater. The tests of these propellers reveal the effect of changes in solidity resulting either from increasing the number of blades or from increasing the blade width.

It was found that (1) increasing the solidity by adding blades had a lesser adverse effect than increasing it by increasing the blade width; (2) the loss in efficiency commonly conceived to be the result of increasing the number of blades was not fully realized, only about 2 percent difference in peak efficiency between a 2-blade and a 4-blade propeller being measured; and (3) an increase in solidity tended to delay the stall and to increase the efficiency in the take-off range.

Propeller design charts and methods of computing propeller thrust are included.

INTRODUCTION

Propeller theory indicates that, other factors remaining constant, an increase in the total blade area, or solidity, of a propeller will generally result in a loss of efficiency. Despite this fact the trend for a number of years has been toward a greater solidity as a result of increases in the power of engines and tip-speed or other limitations on the diameter. The 3-blade propeller is replacing the 2-blade propeller and in some cases, as in high-altitude flying, the 4-blade propeller appears to have a field of use.

Propeller research has lagged somewhat behind the needs of industry, particularly with regard to the need for data on full-scale propellers having modern wide blades and on propellers having more than two blades.

Throughout the first part of 1937 the N. A. C. A. 20-foot wind tunnel was engaged in a rather comprehensive propeller-research program covering several phases of the subject. This report presents the results of the part of the program concerning the effect of number of blades and of blade width on the aerodynamic characteristics of full-scale propellers.

The propellers tested, especially those with Clark Y sections, are typical of many in use today; and the data, which cover a blade-angle range up to 45°, should therefore be useful for design purposes. The data are presented in a form readily usable for the calculation of take-off thrust, and methods of making such calculations for fixed-pitch and controllable propellers are given in an appendix. The data provide a good comparison of the performances of propellers having Clark Y and R. A. F. 6 airfoil sections, but no point is made of this comparison here because another report dealing specifically with the effect of airfoil sections is in preparation.

APPARATUS AND METHODS

Tunnel.—The tests were made in the N. A. C. A. 20-foot wind tunnel described in reference 1. The tunnel has an open throat and is capable of producing air speeds up to 110 miles per hour.

Propellers.—The seven propellers tested may be classified as follows:

1. A group composed of three propellers having Clark Y airfoil sections with 2, 3, and 4 blades.

2. A group composed of three propellers having R. A. F. 6 airfoil sections with 2, 3, and 4 blades.

3. A single specially constructed propeller similar to the 2-blade propeller of class 2 except that its blade width and thickness are 50 percent greater.

All the propellers have 10-foot diameters and, except for the special wide one, have the same plan form, thickness, width, and pitch distribution. The normal-width propellers are all of Navy design and have drawing numbers 5868–9 and 5868–R6 for the blades of Clark Y and R. A. F. 6 sections, respectively. The wide propeller is of N. A. C. A. design and has an Army drawing number of 37–3647. Its blade width is 50 percent greater than that of the normal-width propeller except the shank, which is the same for both.

Photographs of the normal-width blade and of the special wide blade are shown in figure 1. Figure 2 presents blade-form curves for all propellers and illustrates the differences between the Clark Y and the R. A. F. 6 airfoil sections.

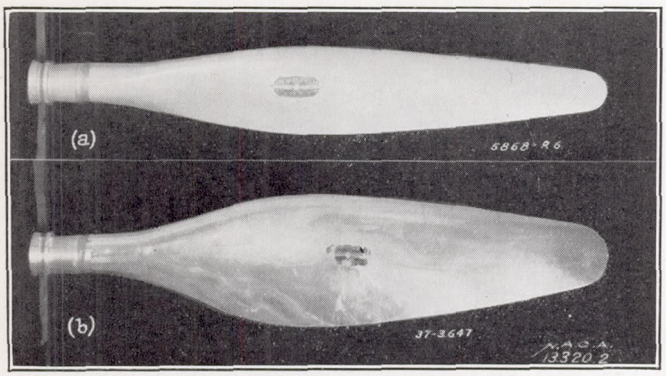

FIGURE 1.—Propeller blades of different width.
(a) R. A. F. 6 blade section of normal width.
(b) R. A. F. 6 blade section 1.5 times normal width.

Body and engine.—The propellers were mounted on a geared Curtiss Conqueror engine enclosed in a smooth liquid-cooled engine nacelle. The engine is rated at 600 horsepower at 2,450 r. p. m. and is geared 7:5. Its direction of rotation had been reversed at the factory to accommodate right-hand propellers.

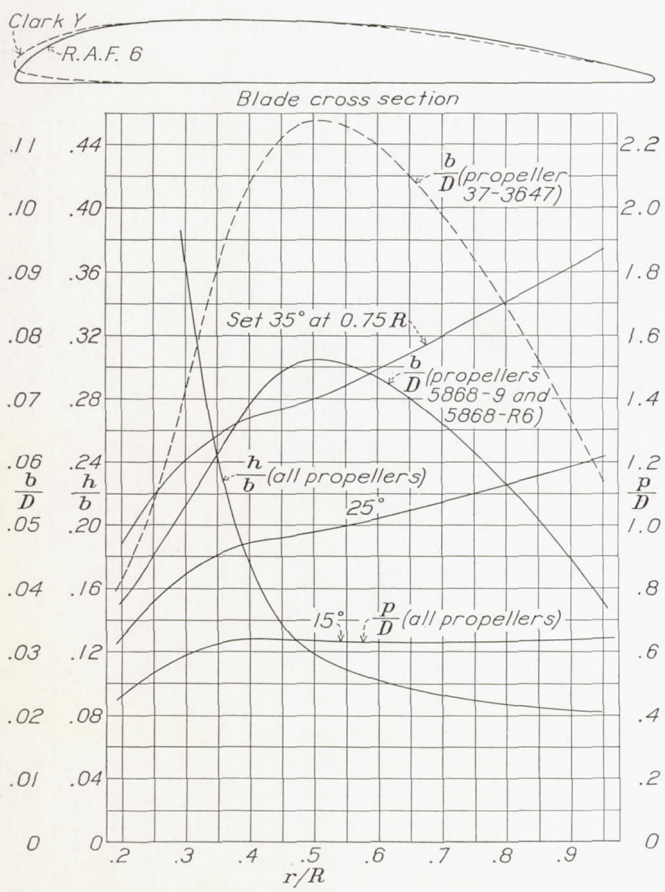

FIGURE 2.—Blade-form curves for propellers 5868–9, 5868–R6, and 37–3647. D, diameter; R, radius to the tip; r, station radius; b, section chord; h, section thickness; p, geometric pitch.

The nacelle is a sheet-metal fairing with oval cross section. Its major dimensions are as follows: maximum depth, 43 inches; maximum width, 38 inches; length, 126 inches. A more detailed description of the nacelle is given in reference 2.

The engine and nacelle were supported on streamline struts rising from the floating frame of the balance system. The drag of the nacelle and struts was about 59 pounds at 100 miles per hour. Figure 3 is a photograph of the nacelle, with propeller, mounted in the tunnel.

Balances, instruments, and torque dynamometer.—The thrust and the torque forces were measured on recording balances situated in the balance house on the test-chamber floor. The torque dynamometer consisted of an engine cradle free to rotate about an axis along one side and supported on the other side by a strut with a footing on the lever mechanism of one of the recording balances on the test-chamber floor. As both the thrust and the torque were measured on recording balances, simultaneous readings were obtained. An electric magneto-type tachometer was used to measure the engine speed.

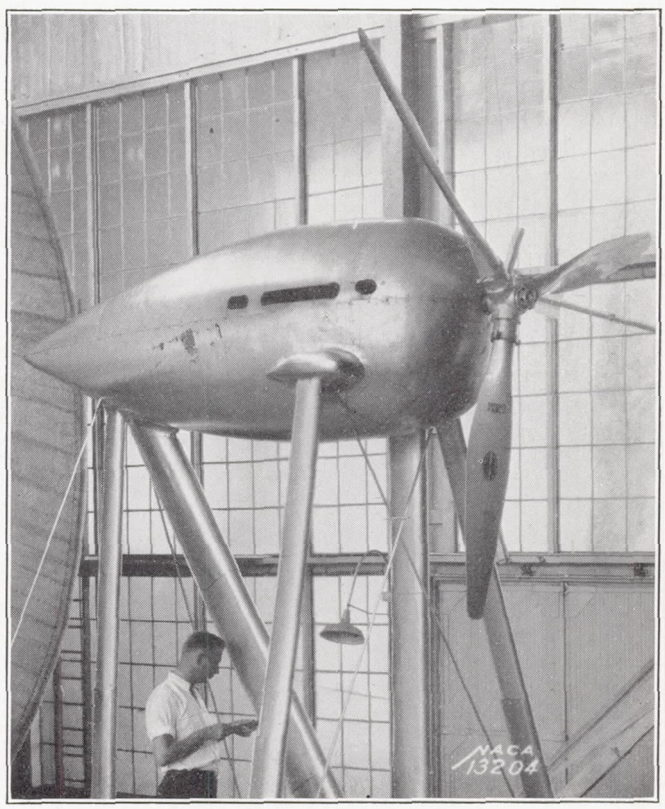

FIGURE 3.—Liquid-cooled engine nacelle and 3-blade propeller mounted in the 20-foot wind tunnel.

Test methods.—The general procedure observed in these tests was to hold the engine speed at a constant value while the tunnel speed was increased by steps to top speed (about 115 miles per hour with propeller operating), after which the tunnel speed was held approximately constant and the engine throttled by steps to zero thrust.

It has been shown in reference 3 that the performance of a propeller in the take-off range is considerably affected by the propeller tip speed. In order to apply the necessary corrections when the present data are used, it is necessary to know the tip speeds of these tests. The following table gives the values of engine speed that were held constant throughout the first part of each test, which covered the take-off and climbing range.

For values of V/nD higher than can be obtained from the table, the test propeller speed may be computed approximately from the relation:

$$\text{r. p. m.}=\frac{1{,}000}{V/nD}$$

Schedule of propeller speeds (revolutions per minute) for tunnel speeds below 115 miles per hour

Propeller \ Blade angle	15°	20°	25°	30°	35°	40°	45°
5868–9, 2 blades	1,200	1,200	1,000	1,000	800	900	800
5868–9, 3 blades	1,000	1,000	1,000	900	800	800	700
5868–9, 4 blades	1,000	1,000	900	800	700	700	600
5868–R6, 2 blades	1,000	1,000	1,000	1,000	1,000	-------	-------
5868–R6, 3 blades	1,000	1,000	1,000	900	800	800	-------
5868–R6, 4 blades	1,000	1,000	1,000	900	800	-------	-------
37–3647, 2 blades	1,000	1,000	1,000	800	800	-------	-------

Precision.—It is impossible to give any exact values for the accuracy of the tests, and the precision of the measurements was so variable that a discussion of the subject would be confusing and pointless. It may be said, however, that repeat tests usually checked first tests within about 1 percent. Some idea of the precision of the measurements is indicated by the regularity of the test points shown in figure 4. This figure is included only to show the dispersion of the test points.

RESULTS

Propeller charts.—The principal results of the tests are presented in figures 5 to 32. These figures present the basic curves of C_T, C_P, η, and C_s against V/nD traced from the original curves of faired test points. The test results have been tabulated in seven tables, which are available on request from the National Advisory Committee for Aeronautics.

As an aid in calculating the propeller thrust in the take-off and climbing range, lines of constant thrust coefficient have been superimposed on the C_P charts. The method of using these charts is described in the appendix to this report.

Coefficients.—The coefficients are standard forms defined in the cover of every N. A. C. A. report, but the definitions will be repeated here for clearness and convenience.

$$C_T=\frac{T_e}{\rho n^2D^4};\ C_P=\frac{P}{\rho n^3D^5};\ \eta=\frac{C_T}{C_P}\frac{V}{nD}$$

$$C_s=\sqrt[5]{\frac{\rho V^5}{Pn^2}};\ C_Q=\frac{Q}{\rho n^2D^5}$$

where T_e is effective thrust$=T-\Delta D$, lb.

T, tension in propeller shaft, lb.

ΔD, change in drag of body due to slipstream, lb.

P, power absorbed by propeller, ft.-lb./sec.

n, propeller speed, r. p. s.

D, propeller diameter, ft.

ρ, mass density of the air, slugs per cu. ft.

V, air speed, f. p. s.

η, propulsive efficiency of propeller engine unit.

Q, engine torque, lb.-ft.

DISCUSSION

The ideal efficiency of a propeller according to the axial momentum theory may be written

$$\eta_i=\frac{2}{1+V_s/V}$$

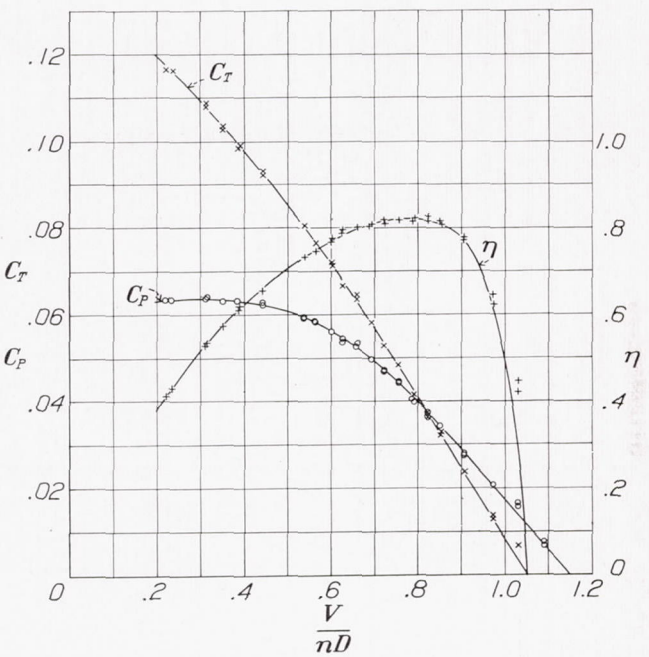

FIGURE 4.—Typical set of test data showing dispersion of test points. Propeller 5868–R6; 2 blades; diameter, 10 ft.; set 20° at 0.75R.

where V_s/V is the ratio of the final slipstream velocity, relative to the airplane, to the forward velocity which, in turn, is defined by the equation

$$\frac{V_s^2}{V^2}=1+2.545C_T/J^2$$

where $J=V/nD$.

It is seen from these equations that, at a given value of J, an increase in C_T increases the slipstream velocity ratio and decreases the propeller efficiency. The two most effective ways of changing C_T are by changing either the blade angle or the solidity. Increasing either the blade angle or the solidity increases C_T so that a decrease in efficiency may be expected. The solidity of a propeller, usually designated by the symbol σ, may be defined as the ratio of the total untwisted blade area to the total propeller-disk area. The solidity is increased by an increase either in the number of blades or in the blade width. An increase in solidity will increase the value of C_T and, therefore, a loss in efficiency may be expected from increasing either the blade width or the number of blades.

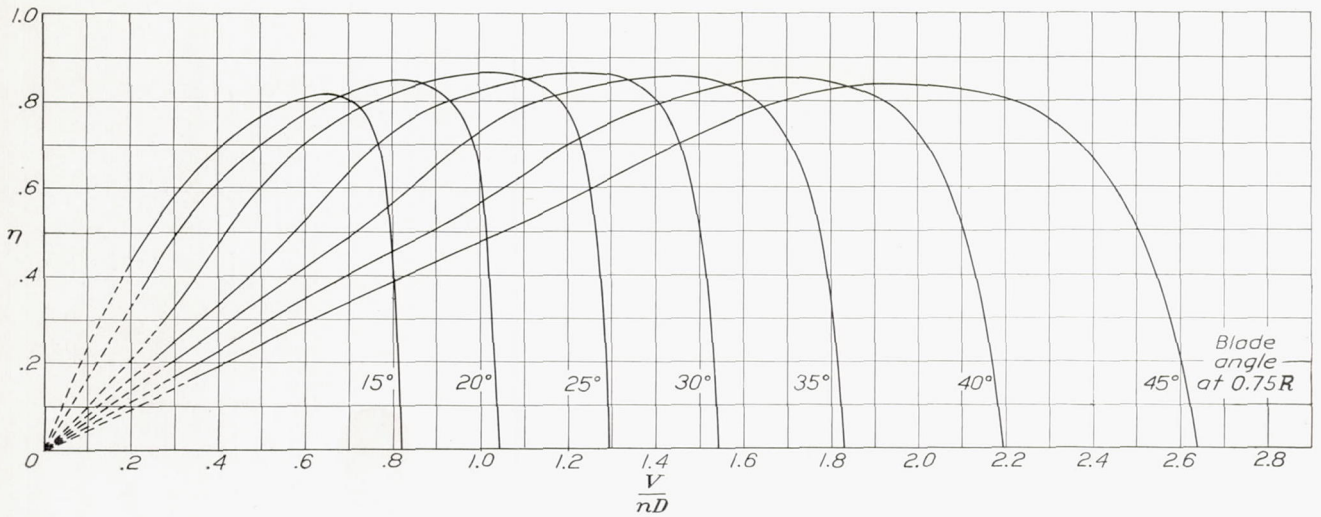

FIGURE 5.— Efficiency curves for propeller 5868-9, Clark Y section, 2 blades.

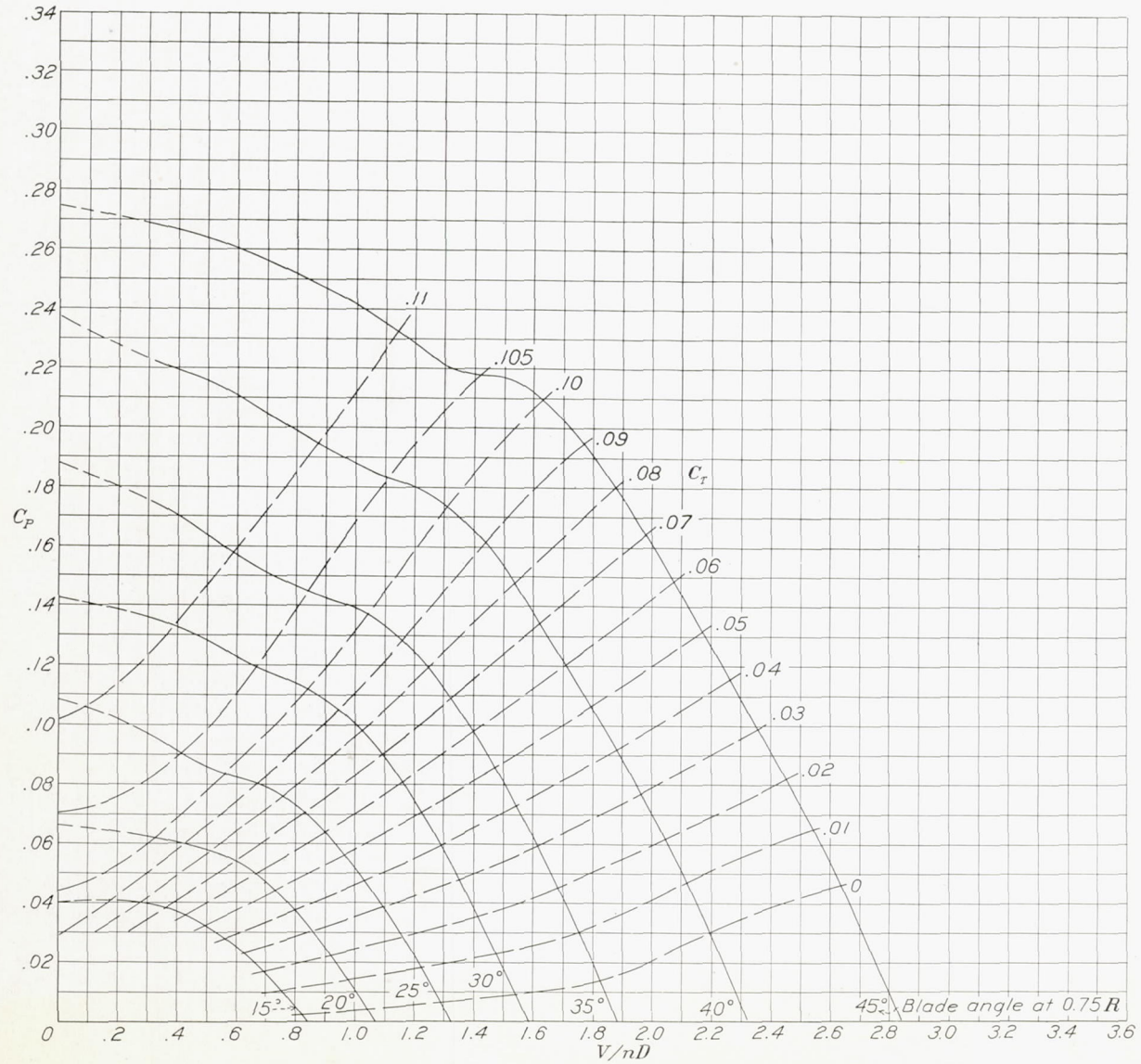

FIGURE 6.—Power-coefficient curves for propeller 5868-9, Clark Y section, 2 blades.

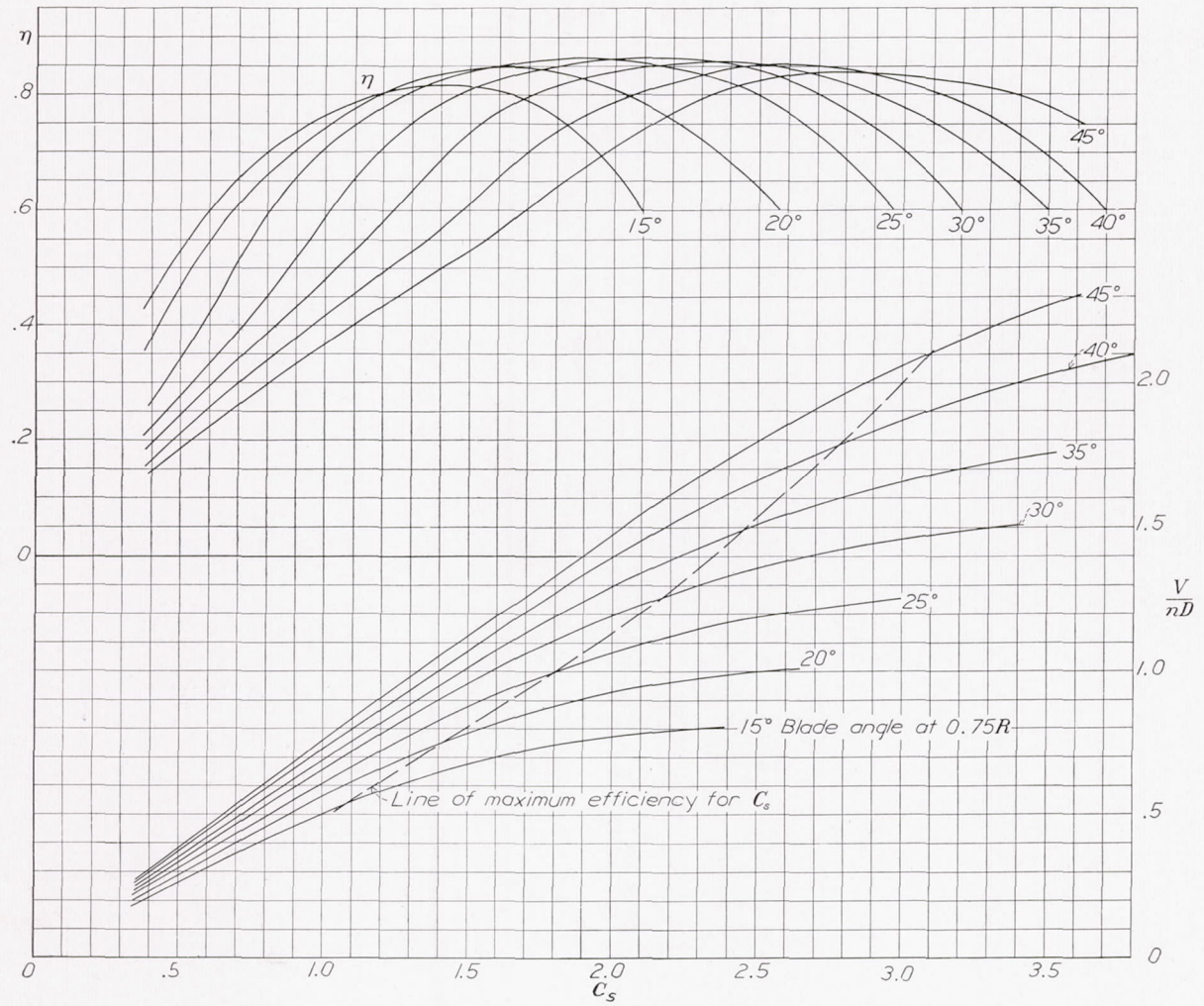

FIGURE 7.—Design chart for propeller 5868–9, Clark Y section, 2 blades.

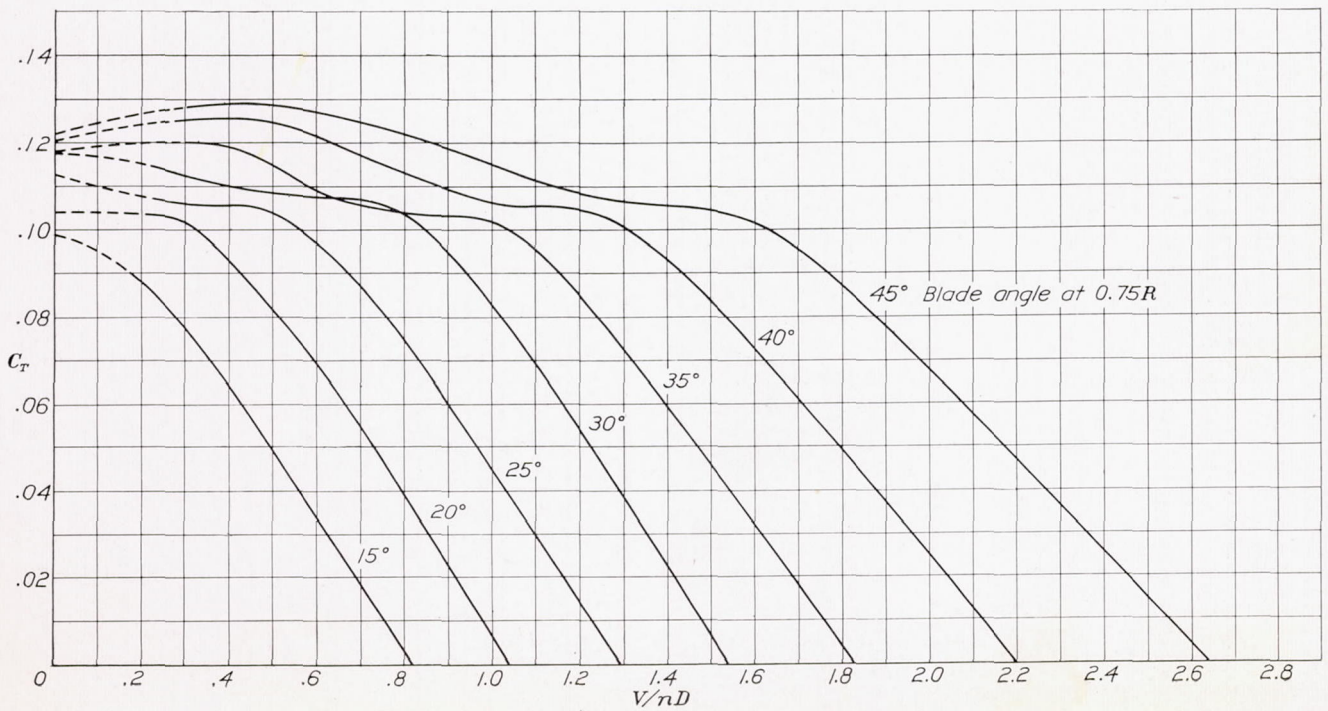

FIGURE 8.—Thrust-coefficient curves for propeller 5868–9, Clark Y section, 2 blades.

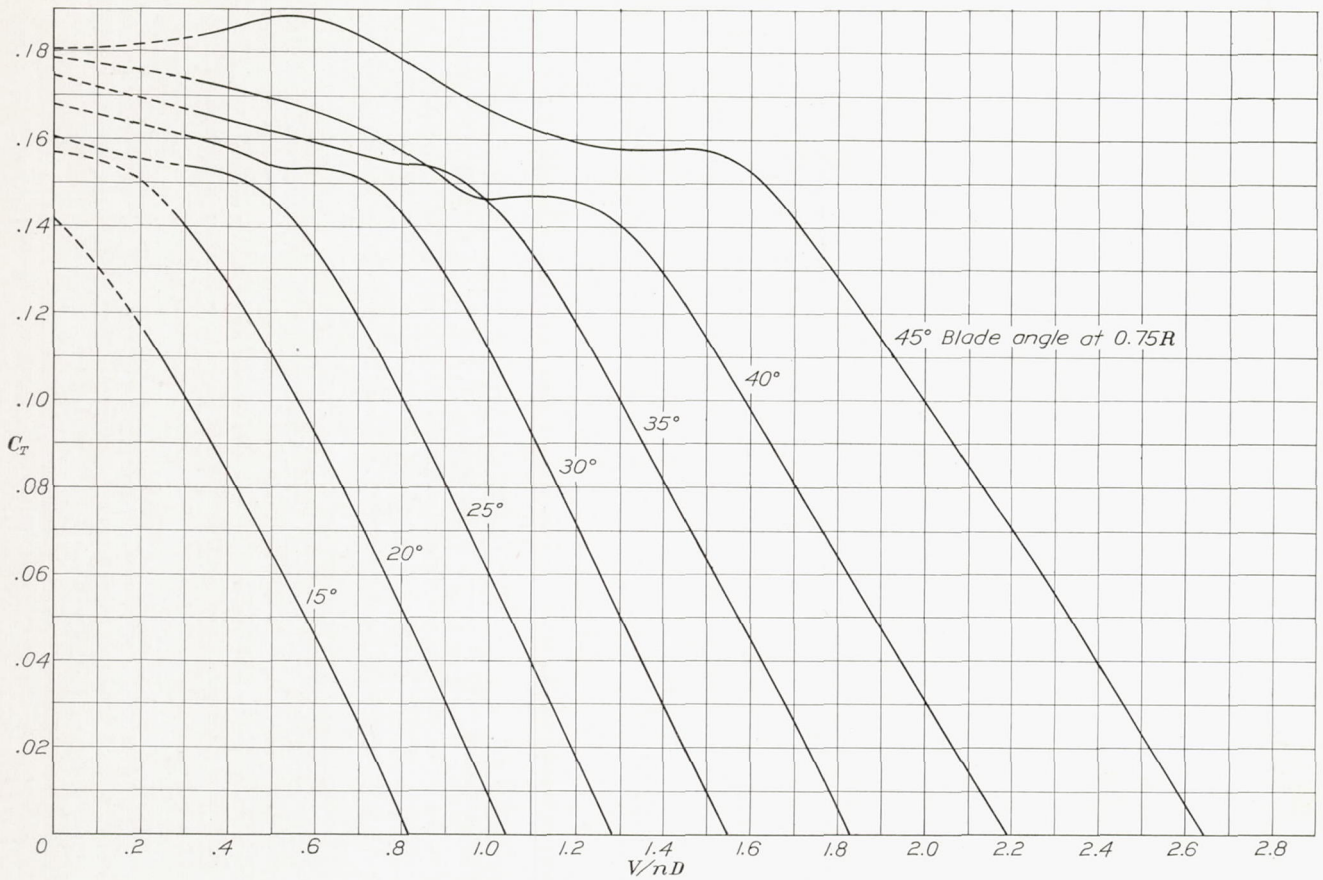

FIGURE 9.—Thrust-coefficient curves for propeller 5868-9, Clark Y section, 3 blades.

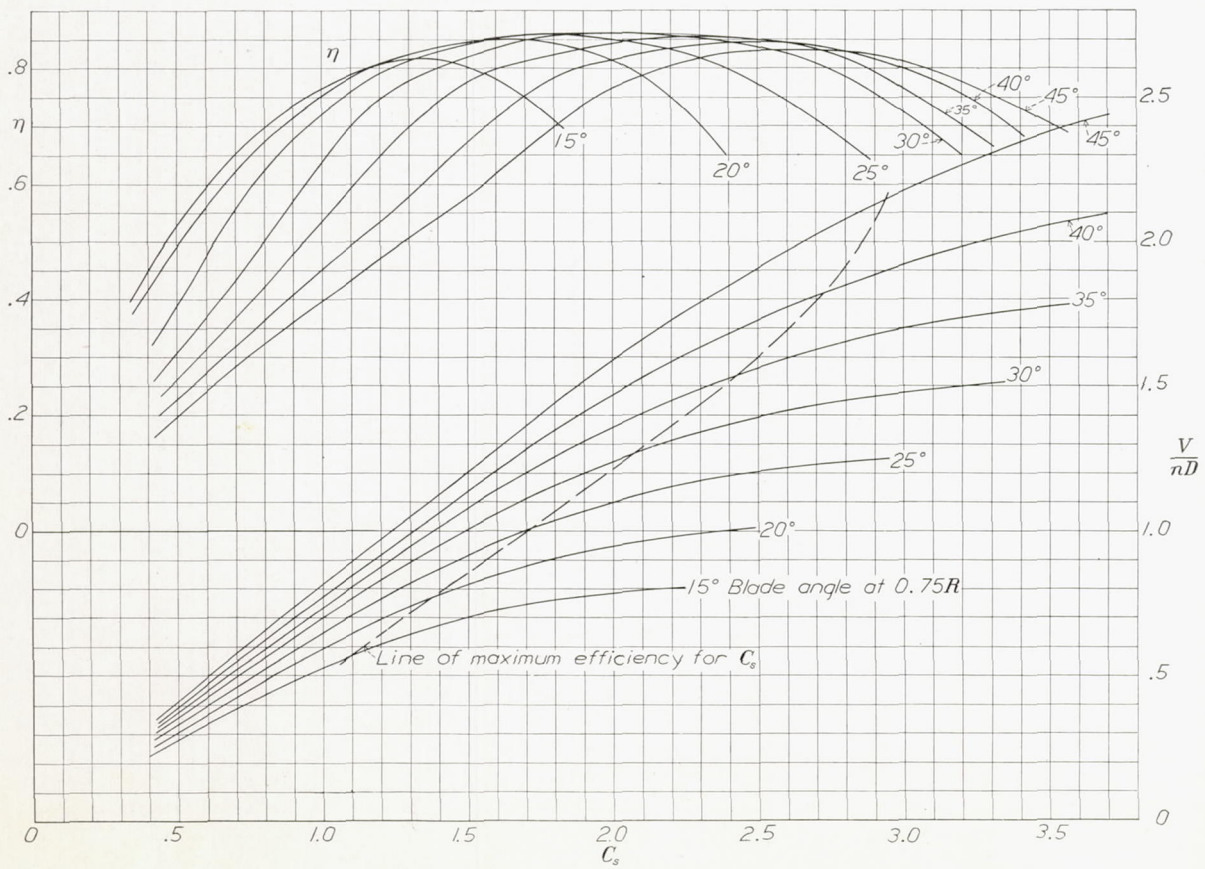

FIGURE 10.—Design chart for propeller 5868-9, Clark Y section, 3 blades.

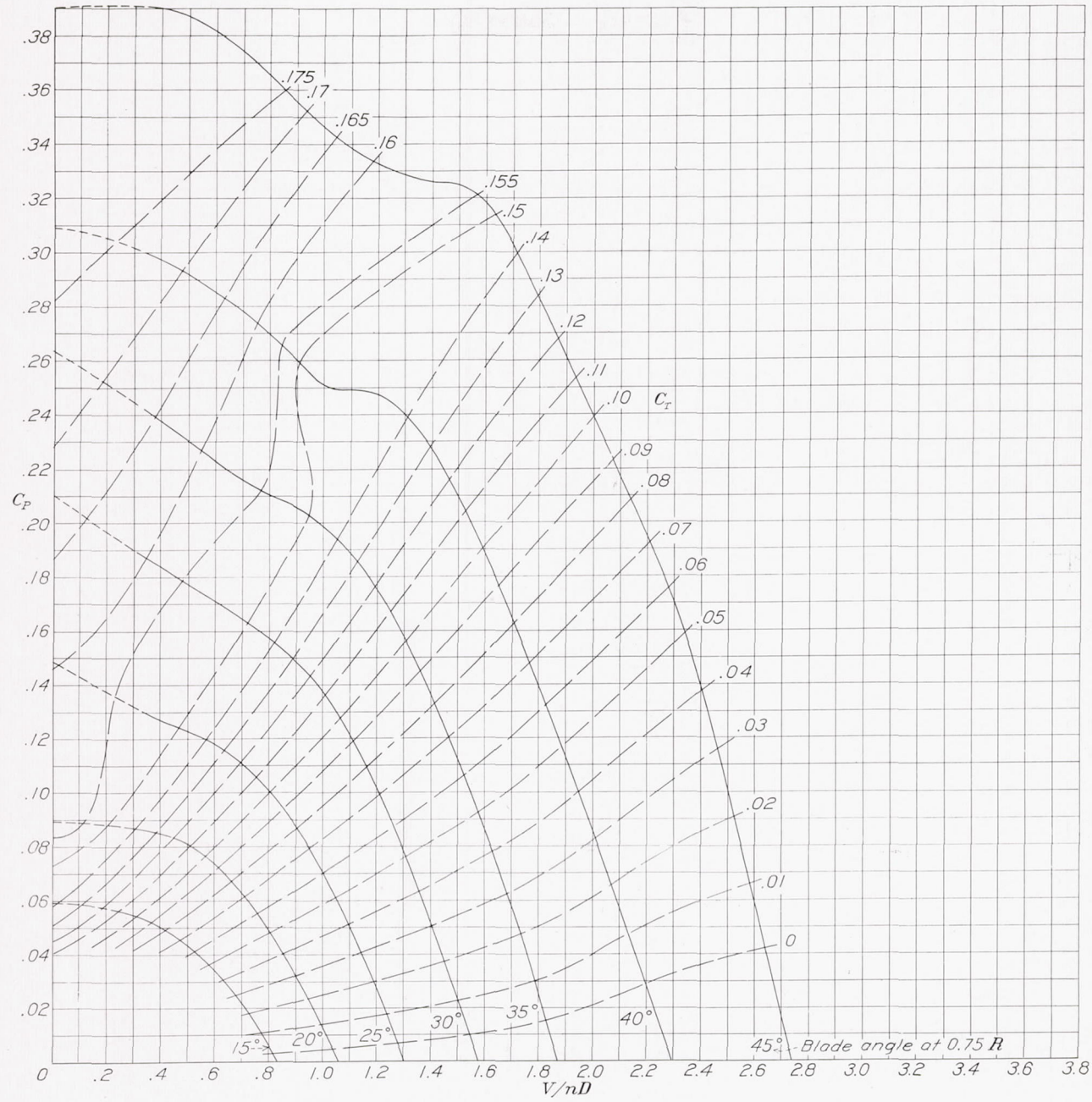

FIGURE 11.—Power-coefficient curves for propeller 5868–9, Clark Y section, 3 blades.

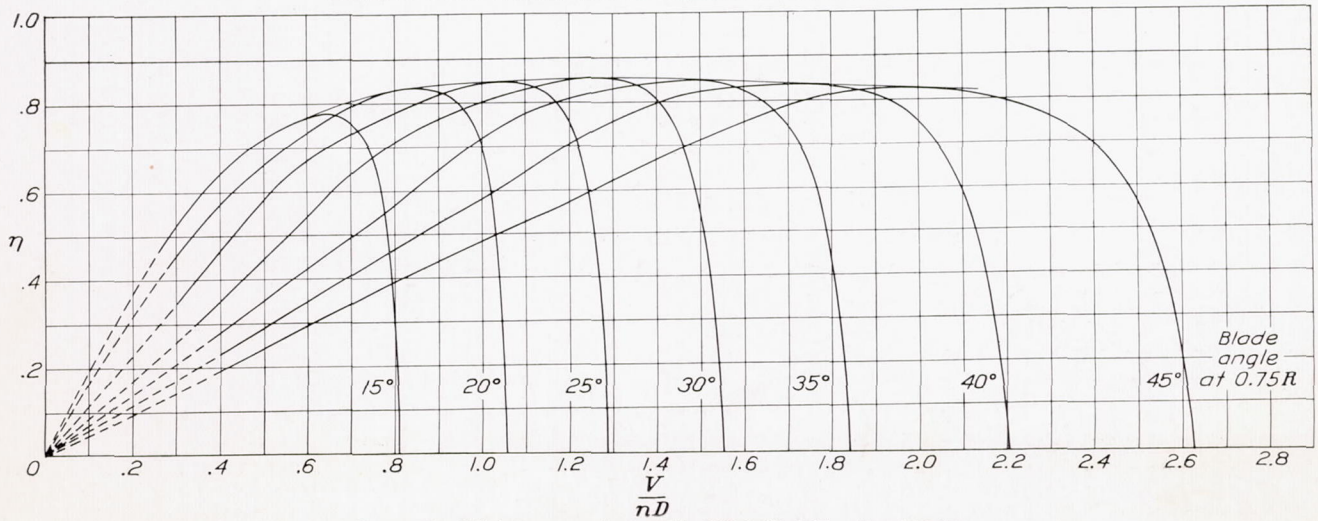

FIGURE 12.—Efficiency curves for propeller 5868–9, Clark Y section, 3 blades.

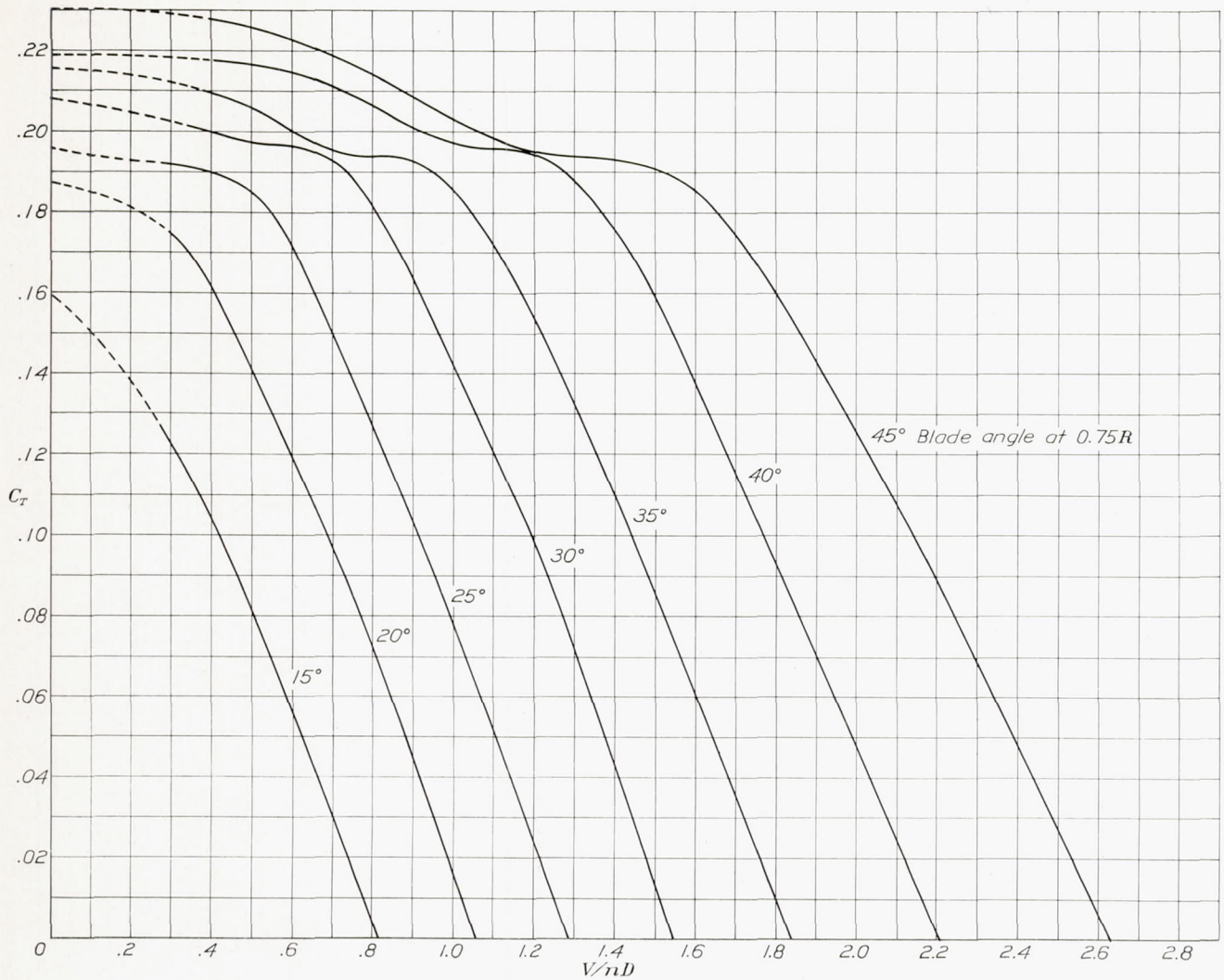

FIGURE 13.—Thrust-coefficient curves for propeller 5868–9, Clark Y section, 4 blades.

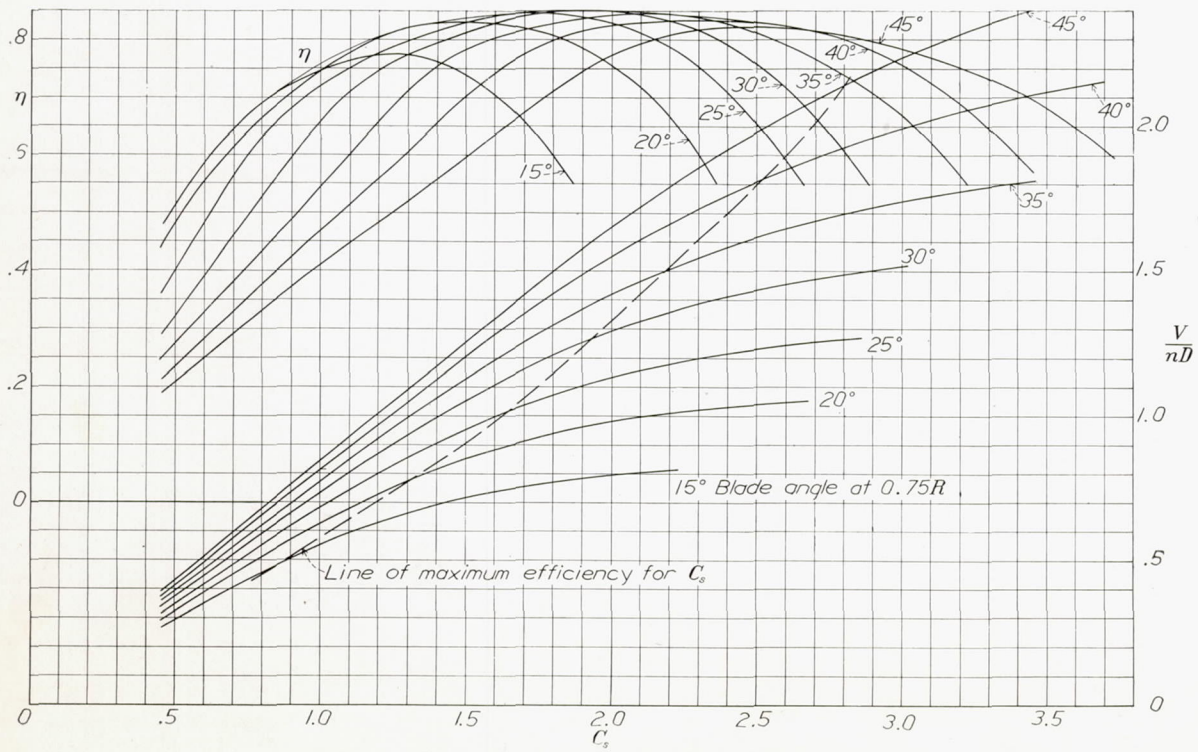

FIGURE 14.—Design chart for propeller 5868–9, Clark Y section, 4 blades.

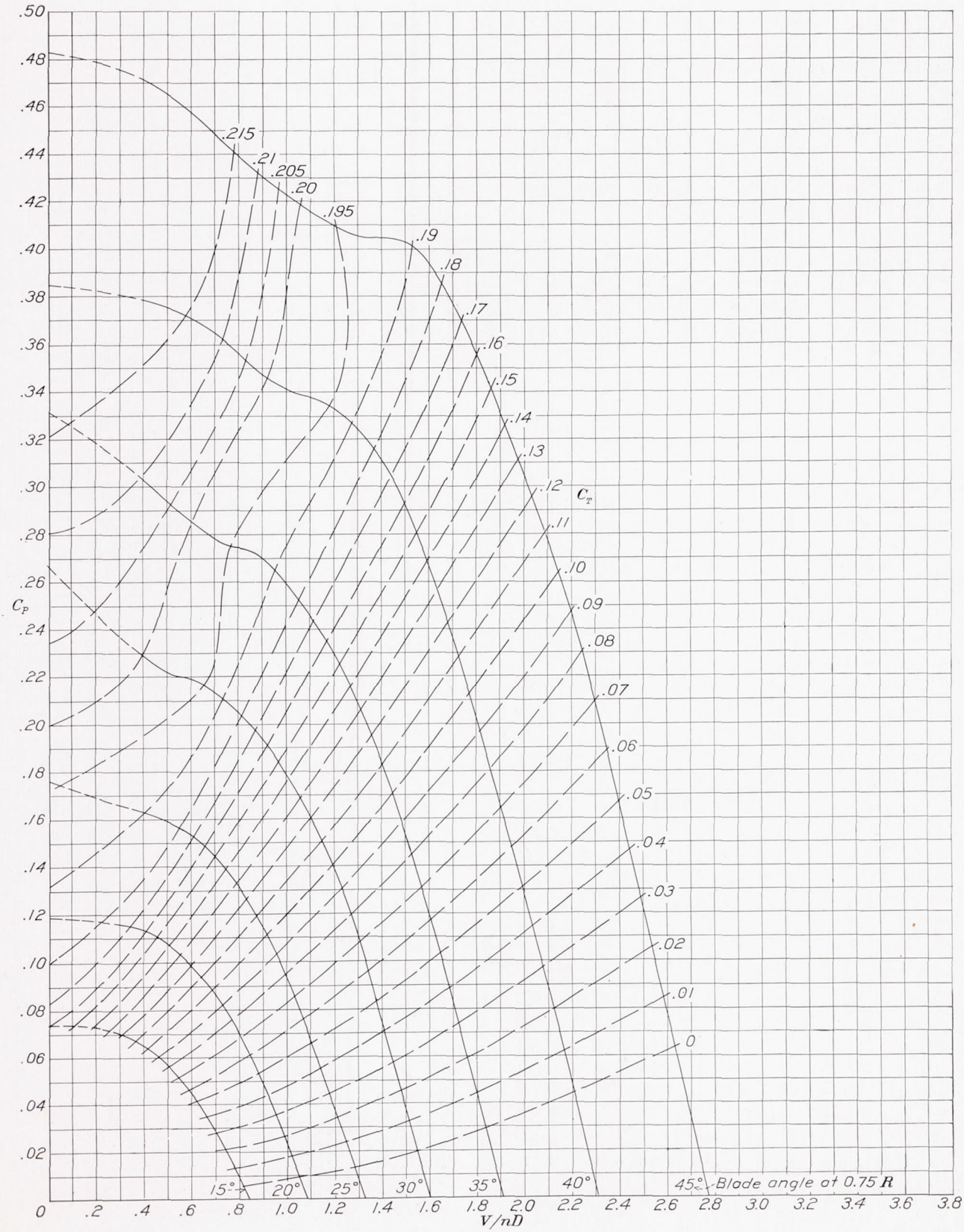

FIGURE 15.—Power-coefficient curves for propeller 5868–9, Clark Y section, 4 blades.

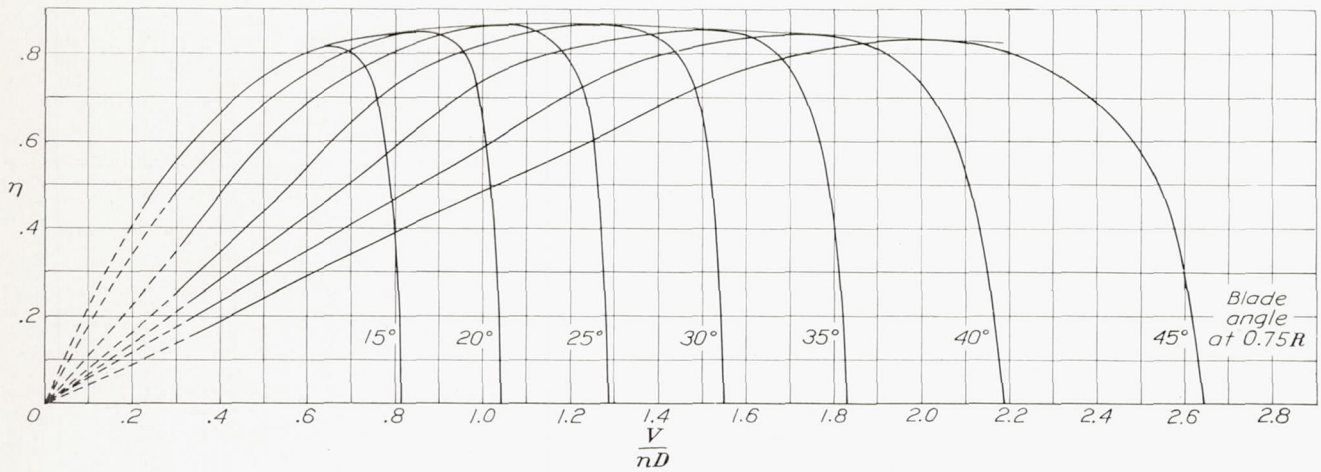

FIGURE 16.—Efficiency curves for propeller 5868–9, Clark Y section, 4 blades.

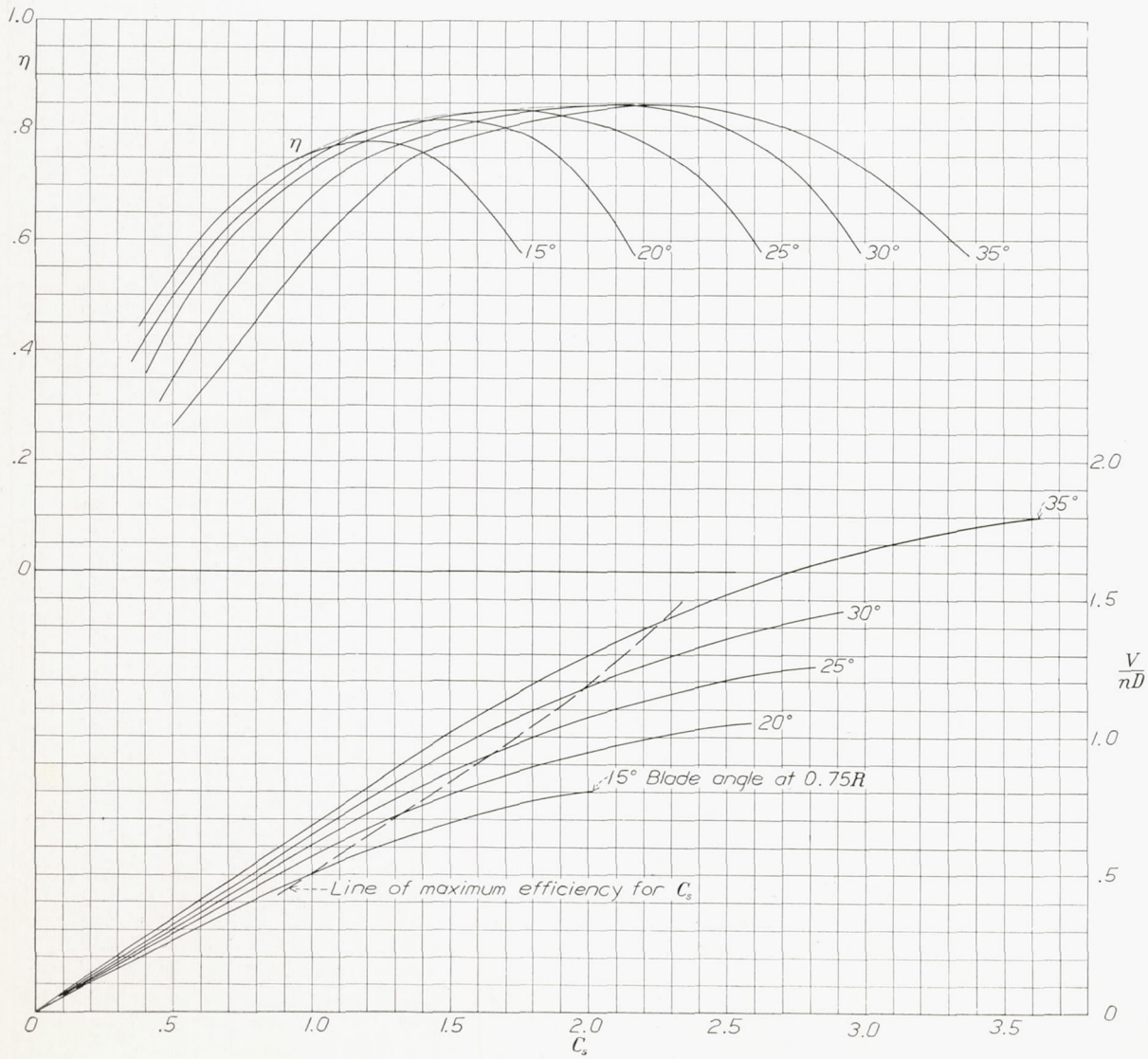

FIGURE 17.—Design chart for propeller 5868–R6, R. A. F. 6 section, 2 blades.

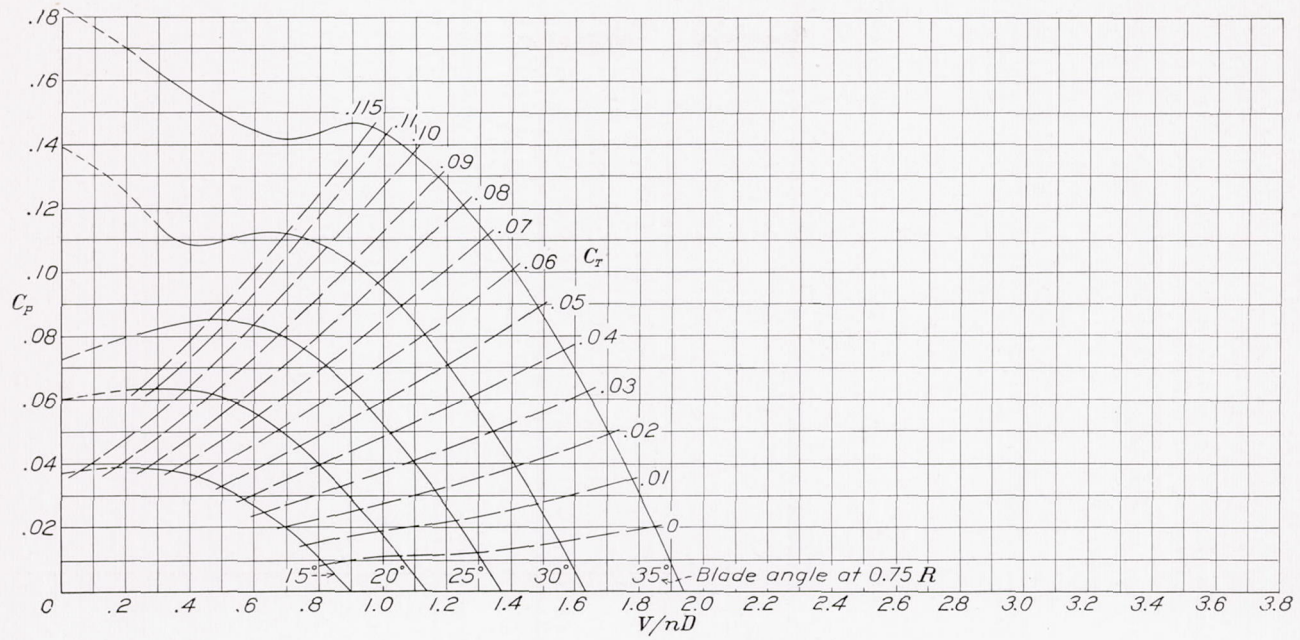

FIGURE 18.—Power-coefficient curves for propeller 5868–R6, R. A. F. 6 section, 2 blades.

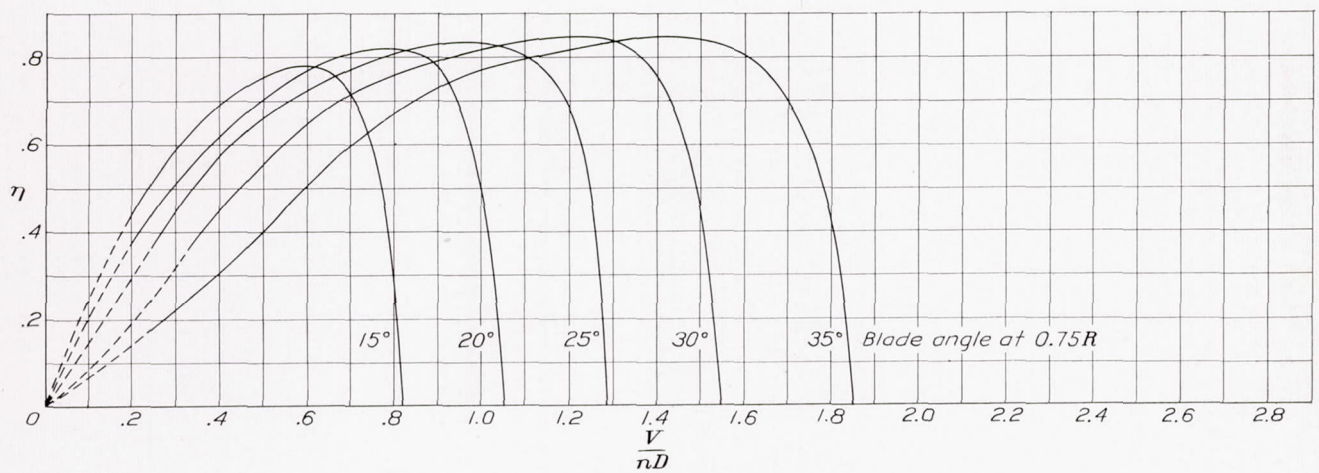

FIGURE 19.—Efficiency curves for propeller 5868–R6, R. A. F. 6 section, 2 blades.

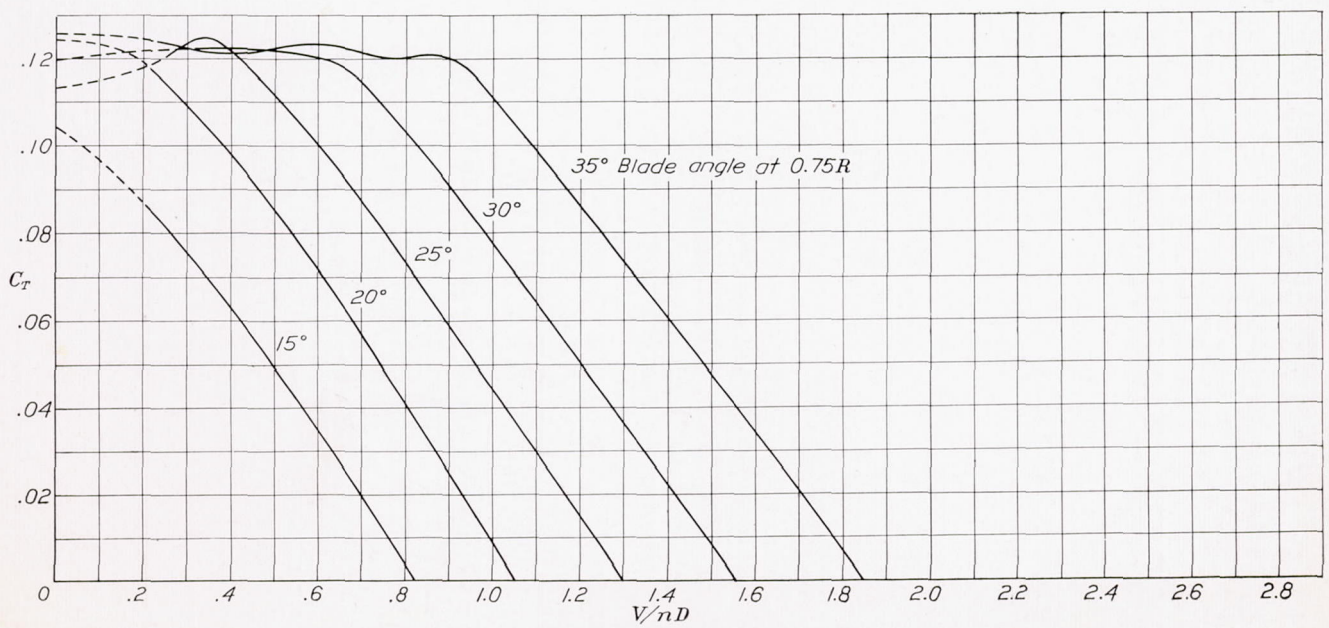

FIGURE 20.—Thrust-coefficient curves for propeller 5868–R6, R. A. F. 6 section, 2 blades.

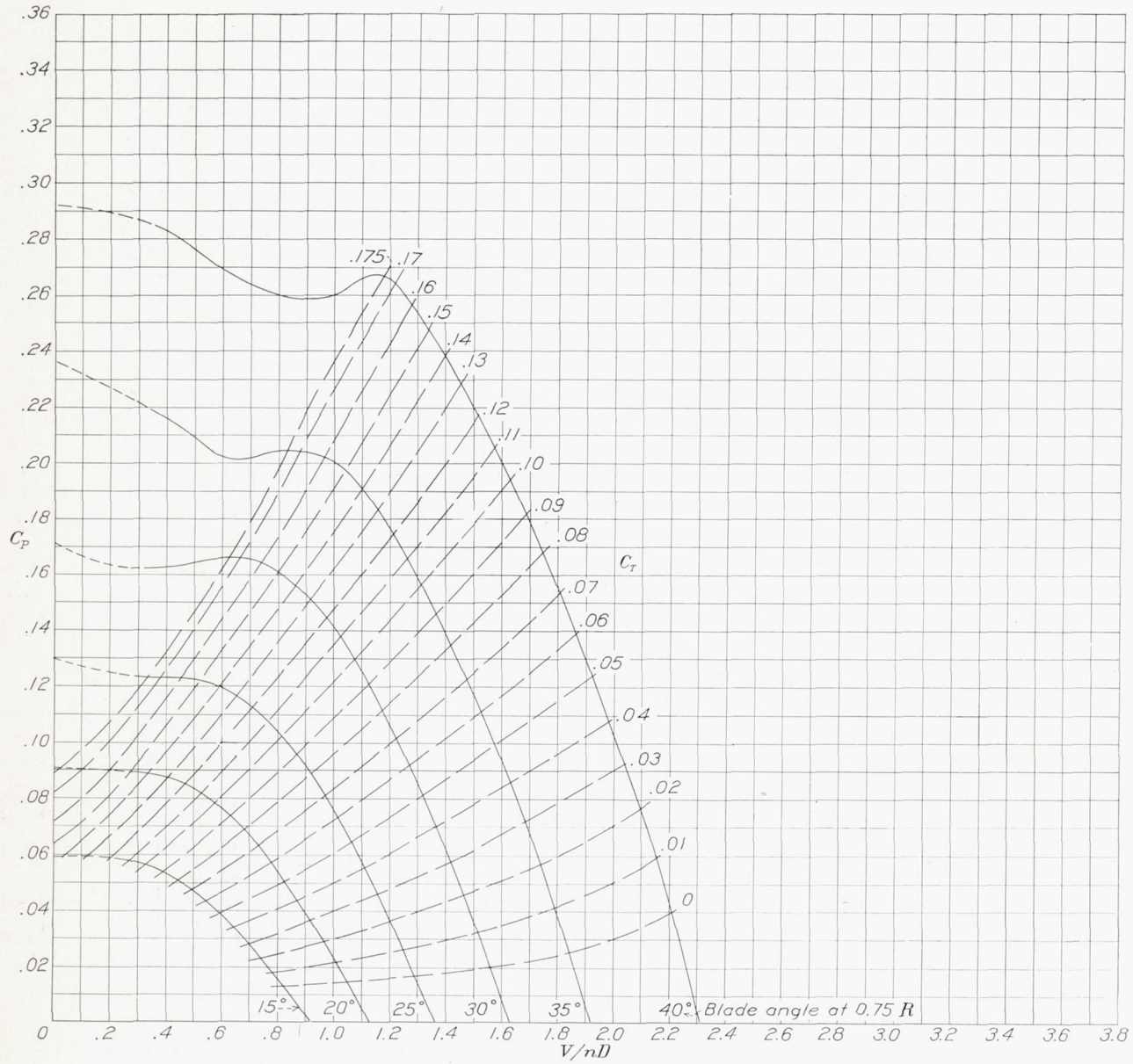

FIGURE 21.—Power-coefficient curves for propeller 5868-R6, R. A. F. 6 section, 3 blades.

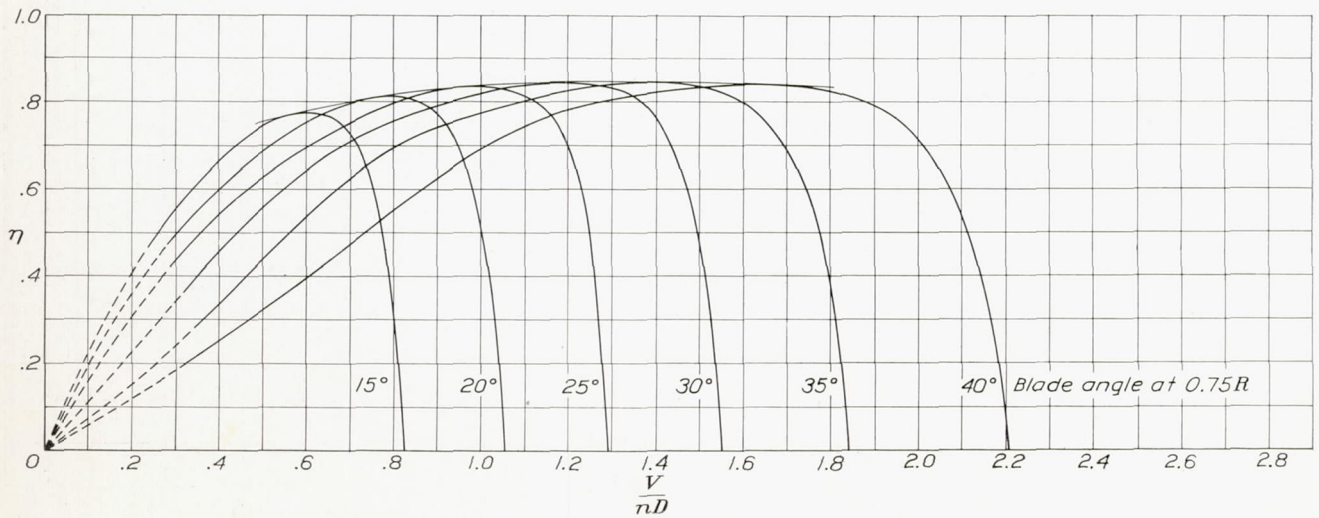

FIGURE 22.—Efficiency curves for propeller 5868-R6, R. A. F. 6 section, 3 blades.

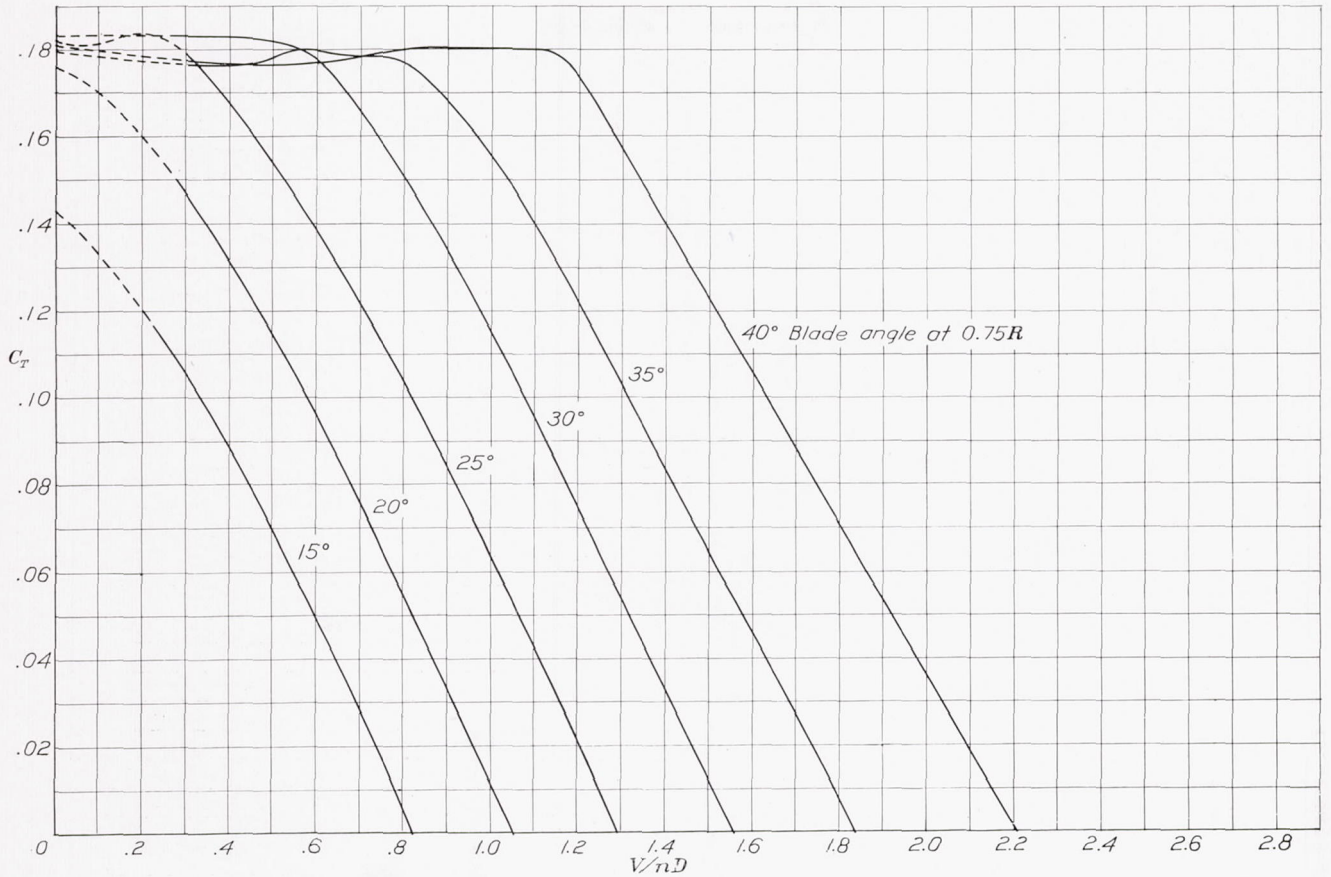

FIGURE 23.—Thrust-coefficient curves for propeller 5868–R6, R. A. F. 6 section, 3 blades.

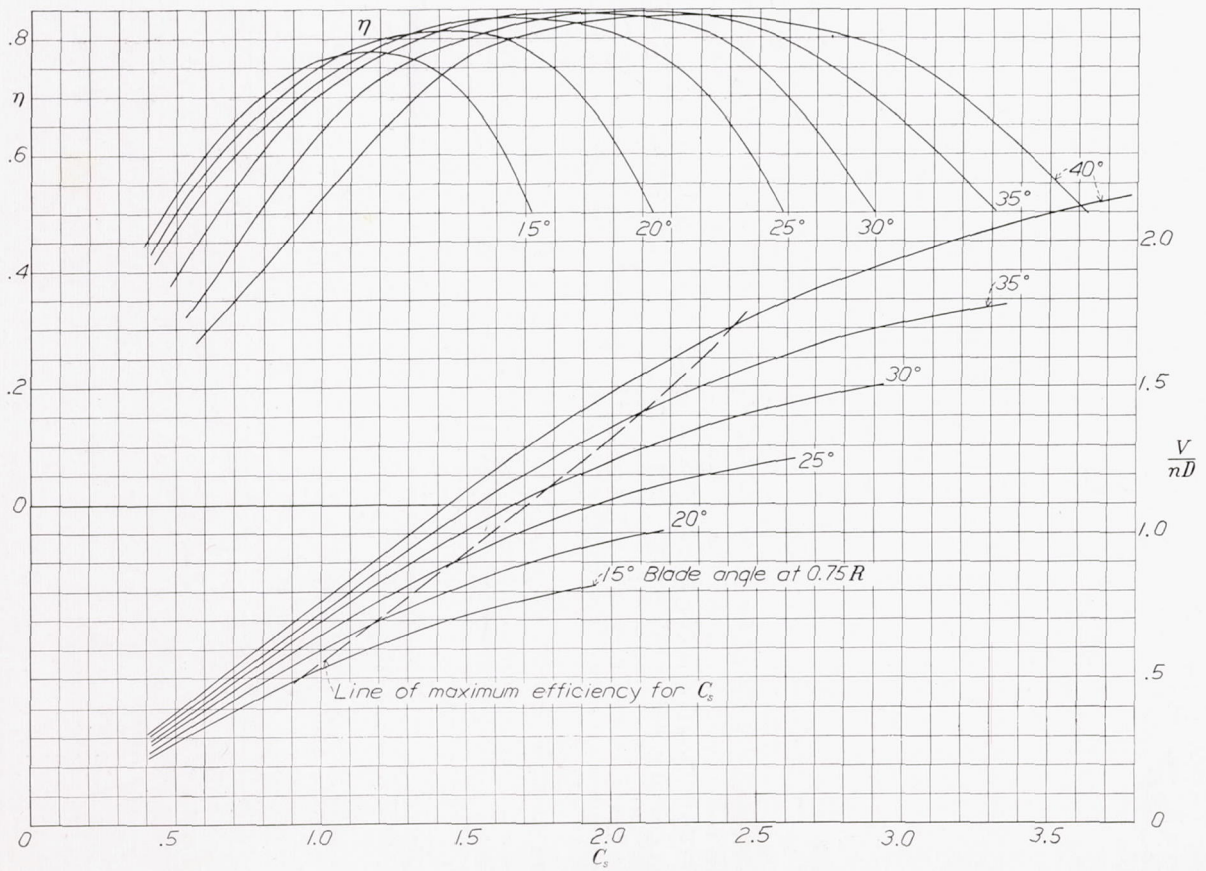

FIGURE 24.—Design chart for propeller 5868–R6, R. A. F. 6 section, 3 blades.

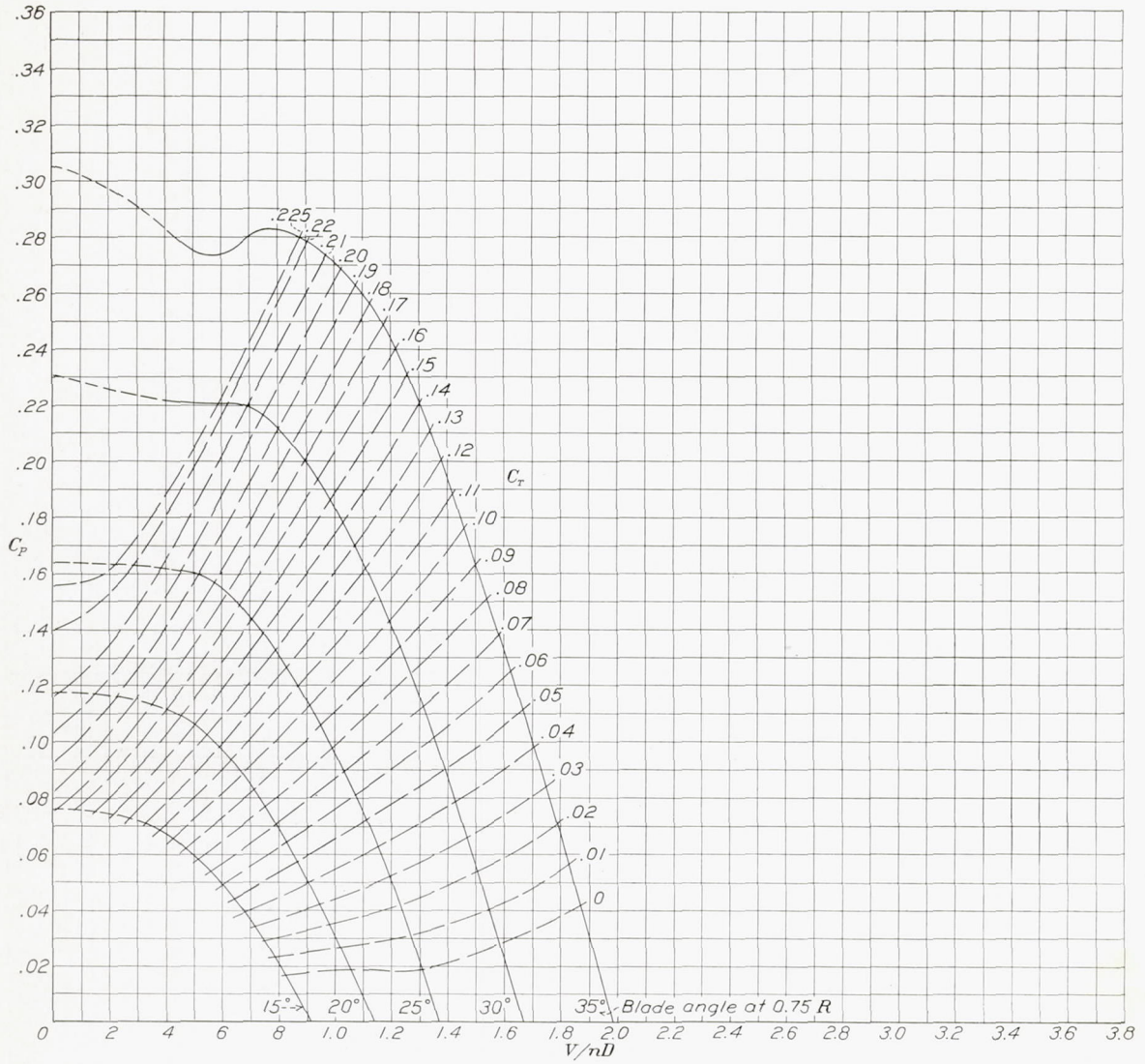

FIGURE 25.—Power-coefficient curves for propeller 5868–R6, R. A. F. 6 section, 4 blades.

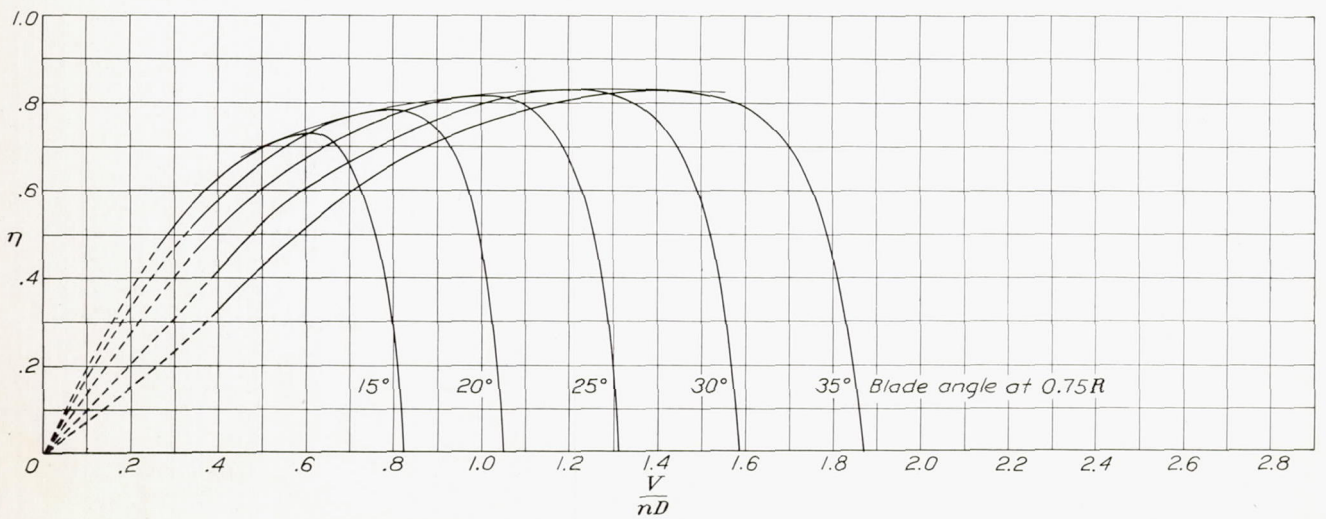

FIGURE 26.—Efficiency curves for propeller 5868–R6, R. A. F. 6 section, 4 blades.

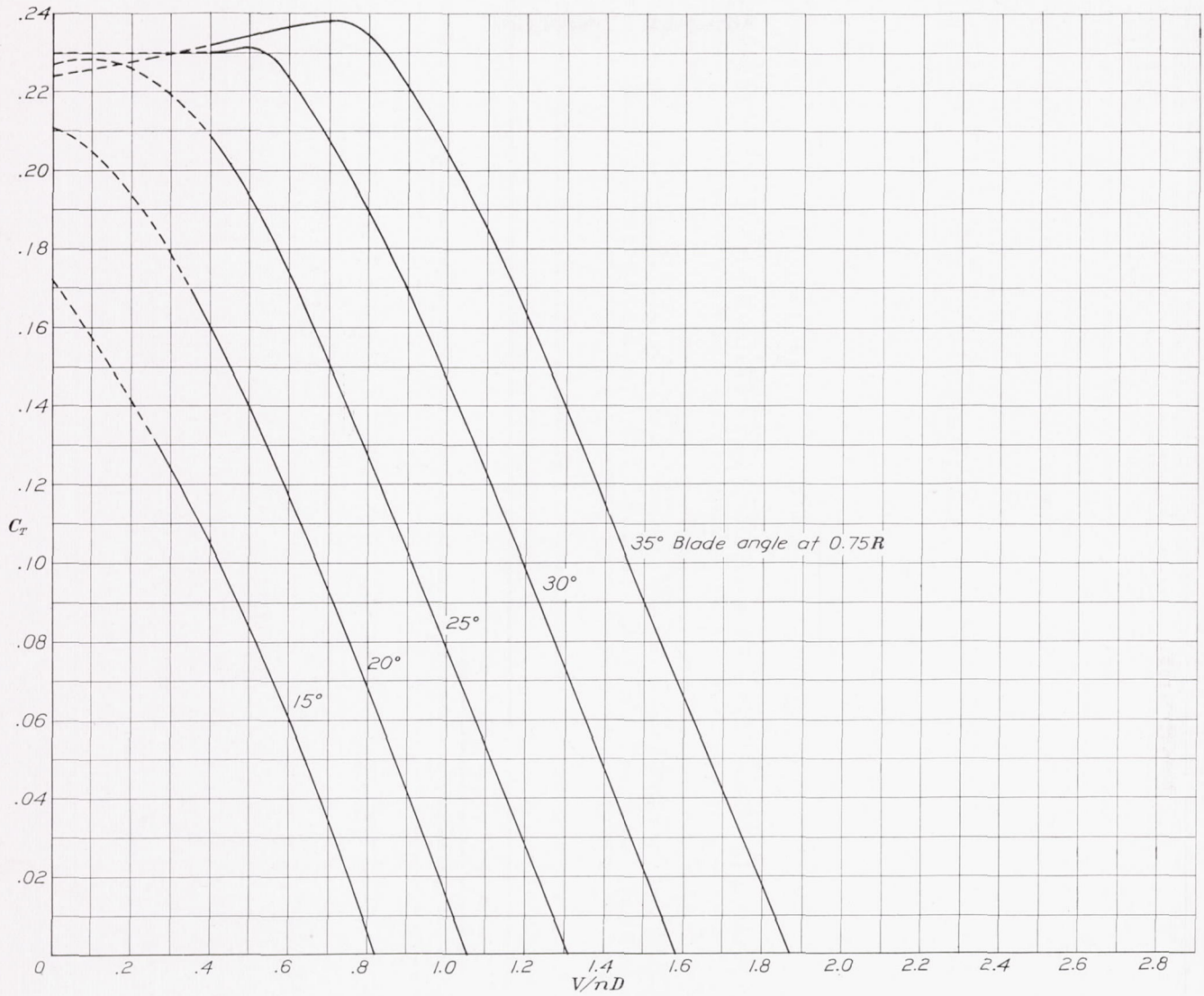

FIGURE 27.—Thrust-coefficient curves for propeller 5868–R6, R. A. F. 6 section, 4 blades.

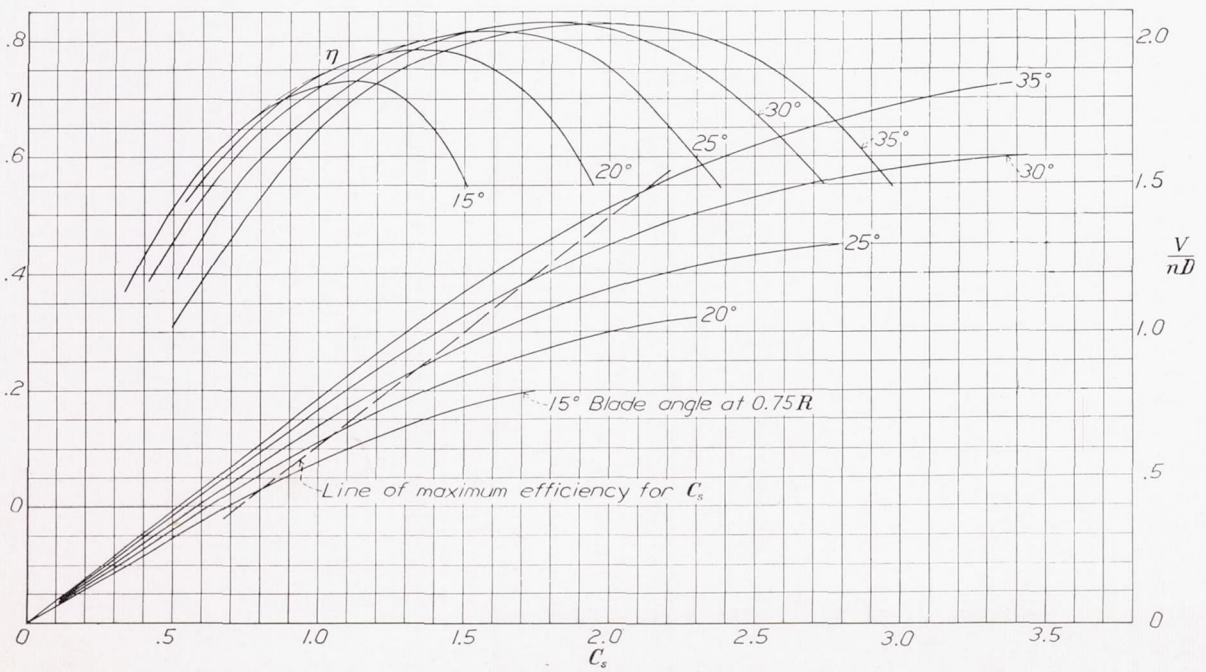

FIGURE 28.—Design chart for propeller 5868–R6, R. A. F. 6 section, 4 blades.

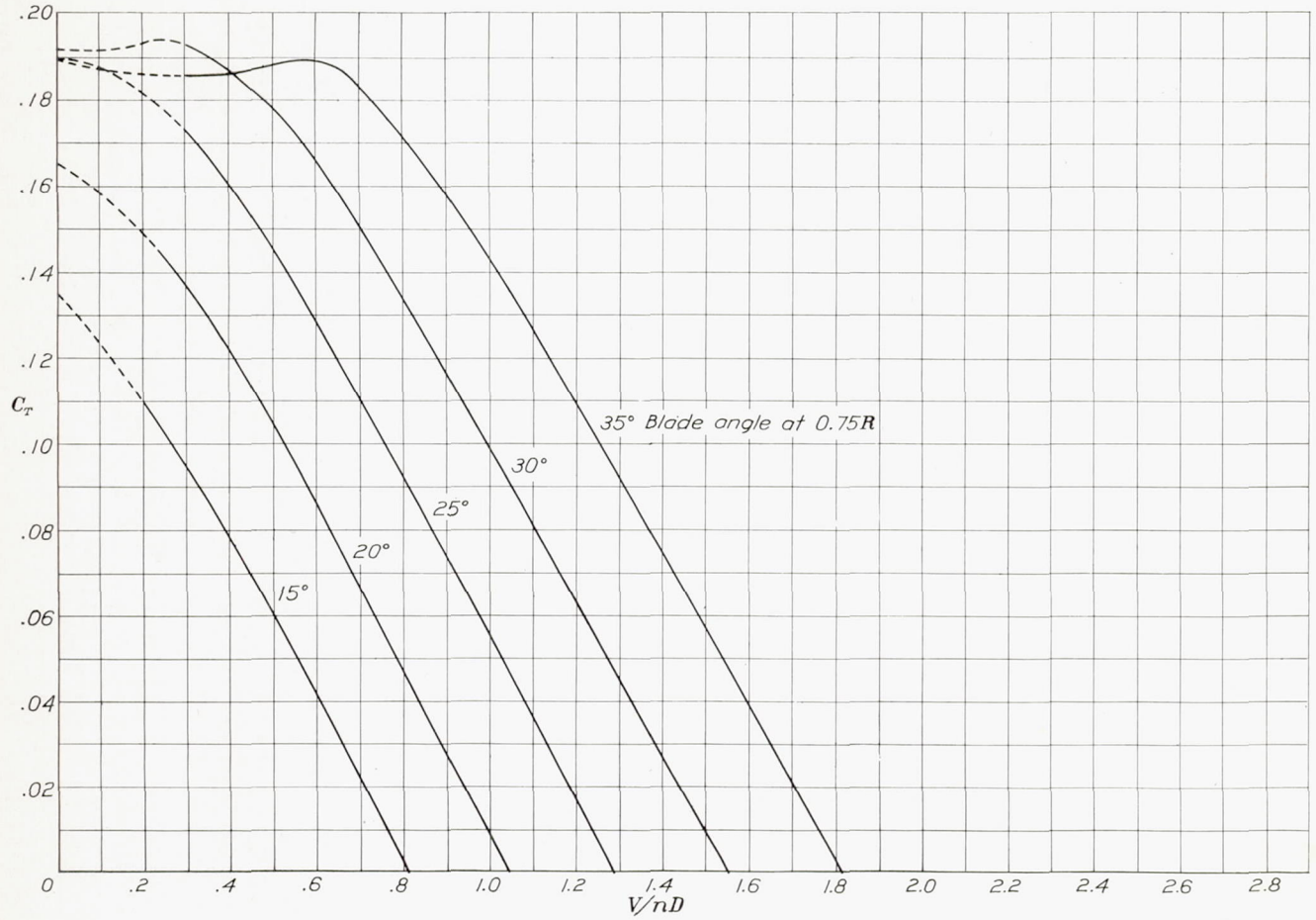

FIGURE 29.—Thrust-coefficient curves for propeller 37-3647, R. A. F. 6 section, 2 blades.

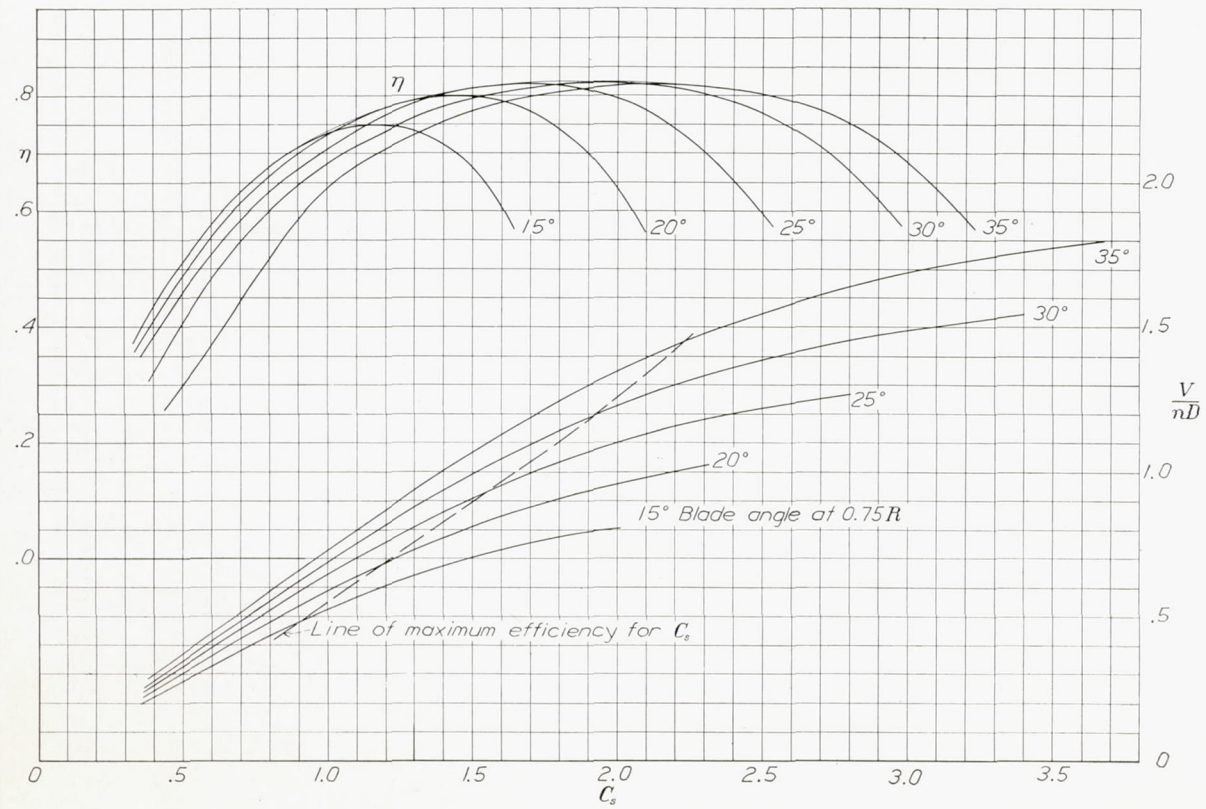

FIGURE 30.—Design chart for propeller 37-3647, R. A. F. 6 section, 2 blades.

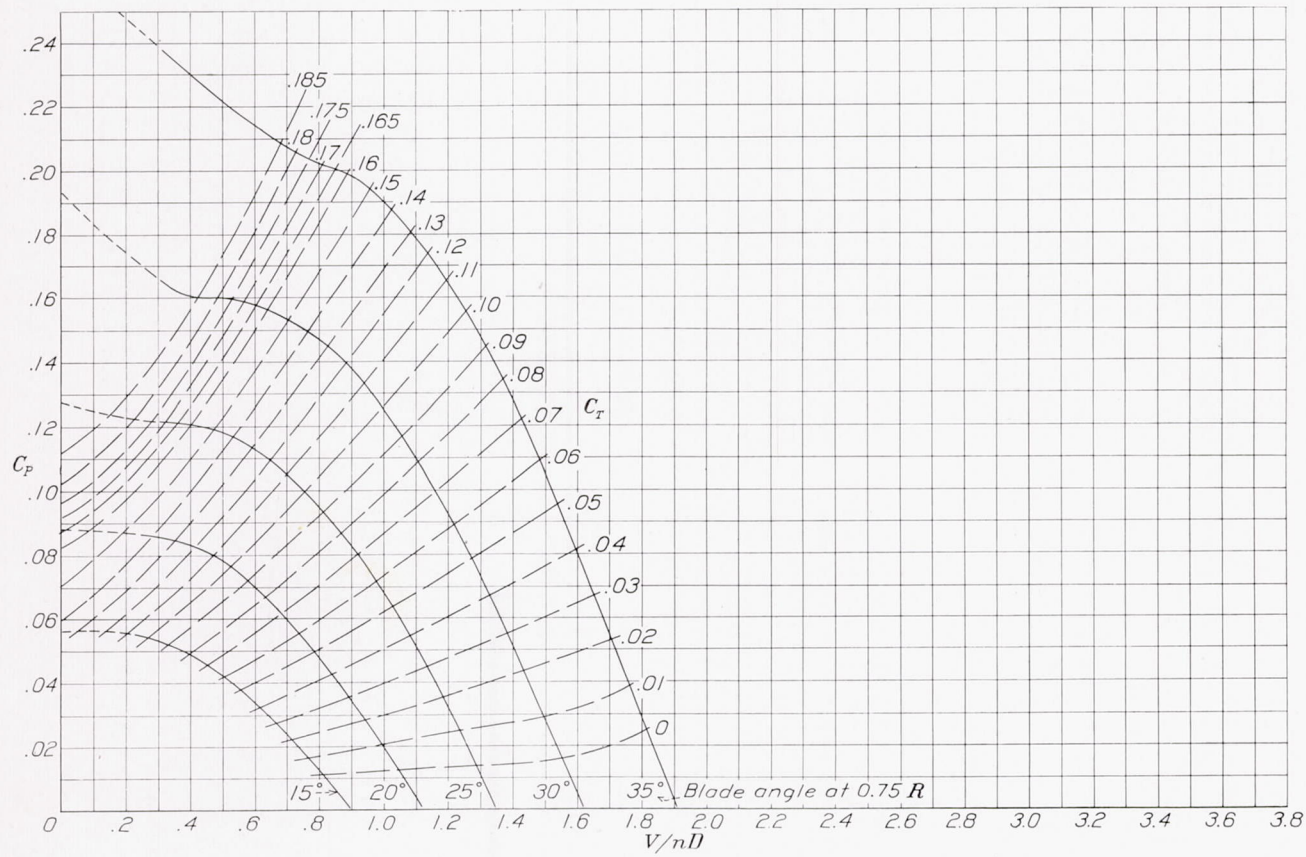

FIGURE 31.—Power-coefficient curves for propeller 37-3647, R. A. F. 6 section, 2 blades.

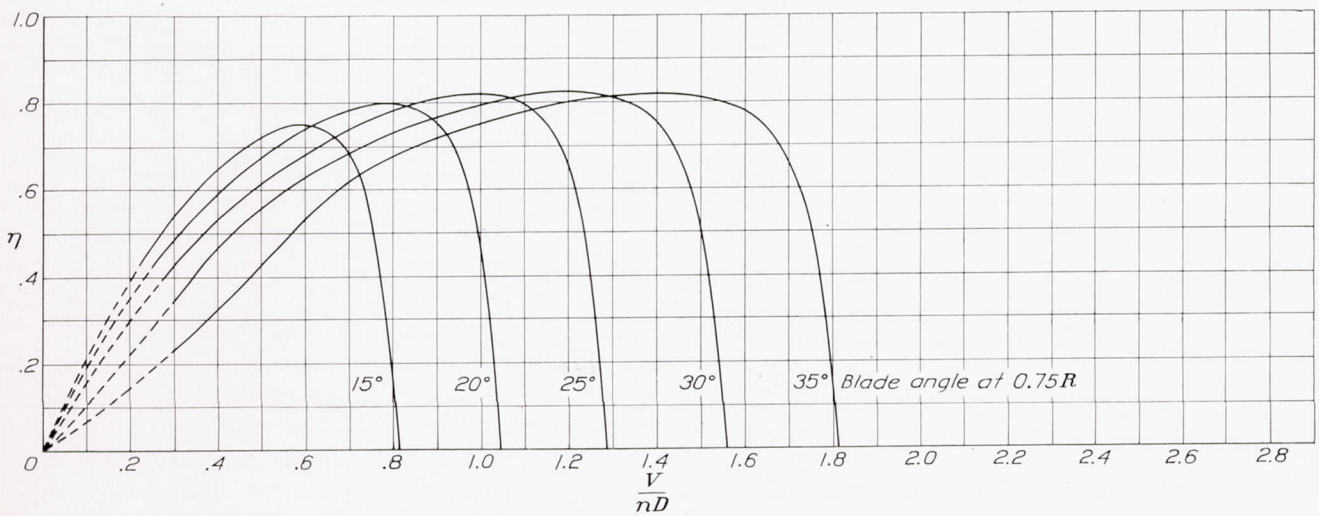

FIGURE 32.—Efficiency curves for propeller 37-3647, R. A. F. 6 section, 2 blades.

At peak efficiency the value of the ratio C_T/J^2 decreases with blade angle, so that the loss in peak efficiency caused by an increase of solidity may be expected to be less at the higher blade angles.

The effect on propeller characteristics of changing the number of blades is illustrated by the C_T, C_P, and η

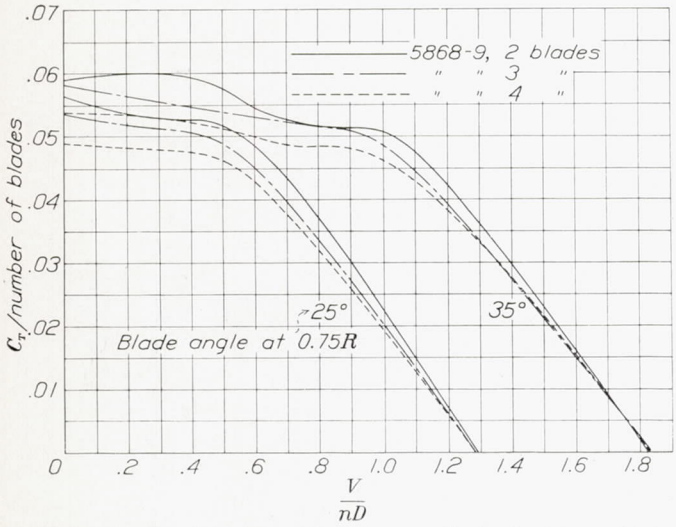

FIGURE 33.—Comparison of thrust coefficients for propellers having 2, 3, and 4 blades.

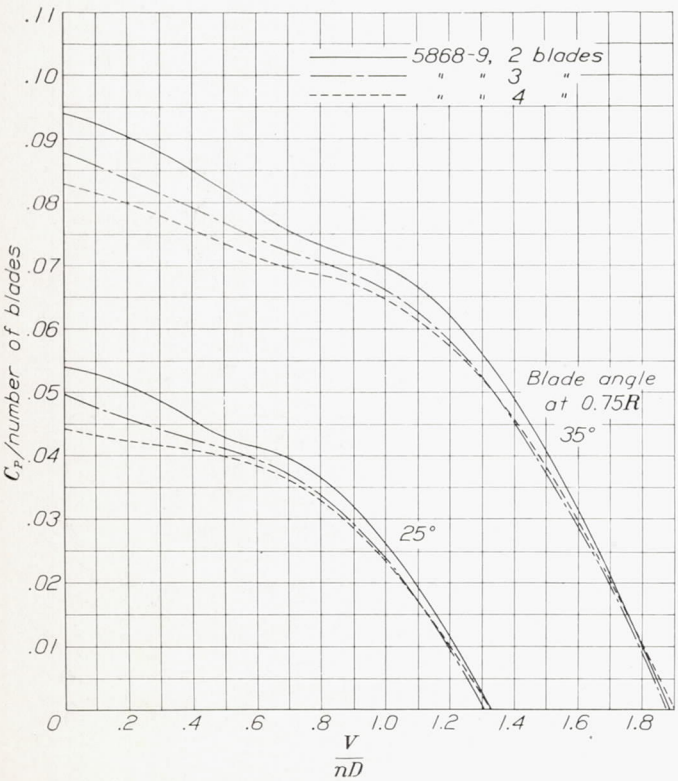

FIGURE 34.—Comparison of power coefficients for propellers having 2, 3, and 4 blades.

curves of figures 33, 34, and 35. Values are given for blade angles of 25° and 35° for all three propellers of Clark Y section.

Owing to the increase in inflow velocity, which theoretically is equal to $(V_s+V)/2$, with increasing number of blades, the thrust-coefficient and power-coefficient curves slope less steeply. The curves come together at $C_T=0$ because here the slipstream velocity becomes zero.

The efficiency curves show a loss for the 3-blade and 4-blade propellers less than would be calculated from the simple momentum theory; in fact, in the portion of the curves where the blades begin to stall, the 3-blade and 4-blade propellers have a somewhat higher efficiency than the 2-blade propeller. The higher efficiency of the 3-blade and 4-blade propellers in the stalled range may be accounted for by the fact that their higher inflow velocities delay and reduce the severity of their stalling.

The effect of a change in solidity has been commonly thought to be the same whether the change results from variation in blade width or number of blades. Modern

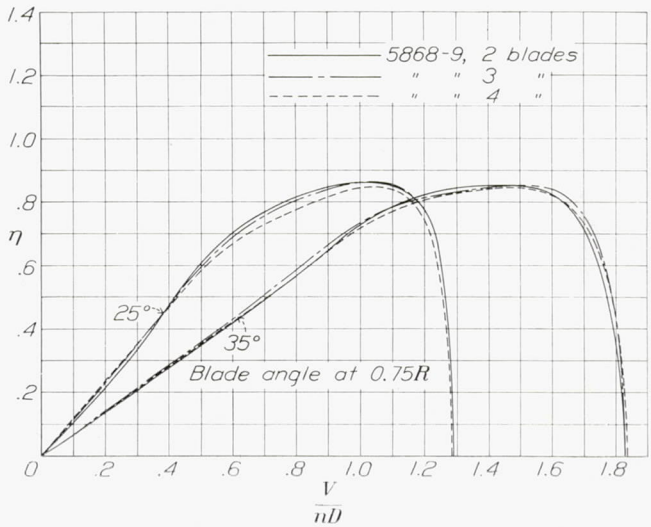

FIGURE 35.—Comparison of efficiency curves for propellers having 2, 3, and 4 blades.

theory and experimental evidence show this belief to be untrue.

The modern vortex theory of propellers pictures each propeller blade, as it describes its helical path through the air, leaving a continuous sheet of vortices behind it which, if no rotational interference velocity is assumed, moves straight backward with slipstream velocity in a manner somewhat similar to the way a screw conveyor appears to move. The strength and backward velocity of the vortex sheets depend on the strength of circulation around the blade itself which, of course, varies with the thrust and therefore with the blade width.

The air trapped between the sheets moves backward with them except for the part that slips forward around the edges of the sheets and produces a tip or edge vortex. The edge vortex destroys some of the circulation of the blade and produces what is known as a "tip loss."

Prandtl has shown (reference 4) that the edge flow, and therefore the tip loss, is reduced if the normal distance between two consecutive vortex sheets is reduced. The distance between vortex sheets is reduced

as the number of blades is increased and, for the ideal propeller with an infinite number of frictionless blades, as postulated in the simple momentum theory, the tip loss becomes zero.

The difference in effect between increasing the solidity

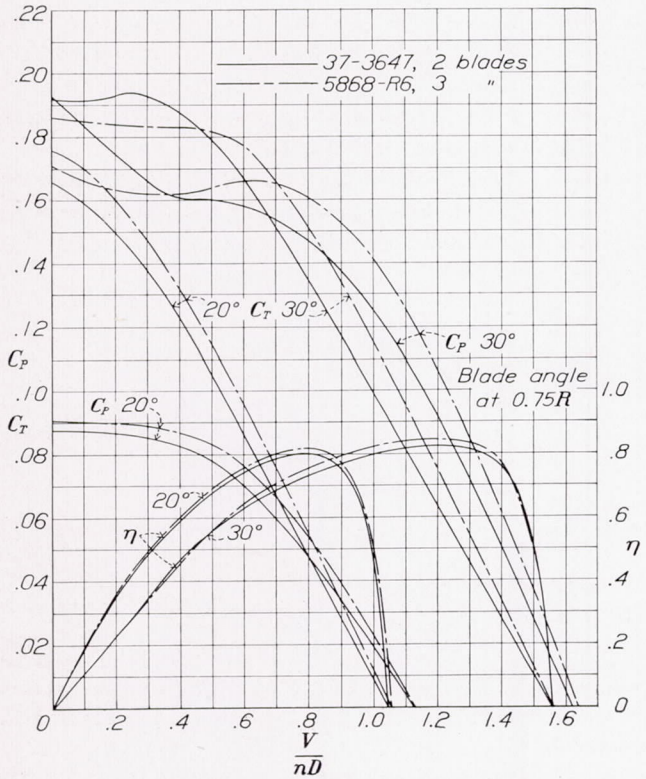

FIGURE 36.—Comparison of propeller coefficients for propellers having the same solidity but a different number of blades.

through the number of blades or through the blade width seems to depend on the following phenomena:

1. Increasing the number of blades decreases the tip loss, which tends to offset the bad effect of the increase in solidity.

2. Increasing the blade width increases the circulation strength around the blade, thus increasing the

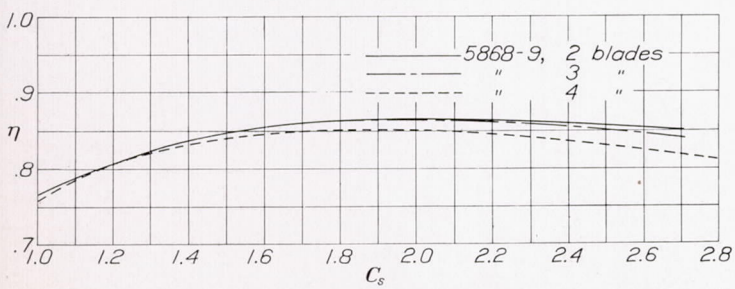

FIGURE 37.—Efficiency-curve envelopes for propellers having 2, 3, and 4 blades of Clark Y section.

local inflow velocity and adding to the bad effect caused by increased solidity.

Some of the results of the present tests, as shown in figure 36, illustrate these effects. In this figure there are shown coefficient curves for a 2-blade and a 3-blade propeller having the same solidity. The propellers have the same diameter, airfoil section, and thickness ratio (h/b), the only difference being that the 2-blade propeller has a blade width 50-percent greater than the 3-blade propeller.

The 2-blade propeller is seen to be distinctly inferior through most of the V/nD range. The increase in local inflow is indicated by the lesser slope of the curves of the coefficients for the 2-blade propeller. It is interesting to note that when the blade stalls, as shown at low values of V/nD on the 30° curves, the power-coefficient, the thrust-coefficient, and the efficiency curves for the 2-blade propeller rise above those for the 3-blade propeller. This result could possibly be attributed to both the higher Reynolds Number at which the 2-blade propeller operated and to the increased inflow of the 2-blade propeller that delayed the stall.

PRACTICAL ASPECTS

From the viewpoint of a designer, it is probably better to compare the performance of propellers, at least their peak efficiencies, on a basis of C_s rather than of V/nD because the coefficient C_s represents the actual design conditions of power, revolution speed, and air speed.

In figures 37 and 38 are presented envelopes of the efficiency curves plotted against the coefficient C_s for the propellers having the Clark Y and the R. A. F. 6 sections, respectively. Each value of C_s represents a certain design condition. Through most of the C_s range for the propellers of both R. A. F. 6 and Clark Y section, the difference between the efficiencies of the 2-blade and 4-blade propellers is 2 percent or less. In both cases, the 3-blade propellers have the same, if not a little higher, efficiency than the 2-blade ones through a large part of the C_s range.

This result seems a bit out of the ordinary but could be explained by the fact that the limits of accuracy of the tests were such as to cause the peak efficiency to vary about 1 percent. The fact that the same condition exists for both the Clark Y and the R. A. F. 6 propellers suggests, however, a legitimacy for the re-

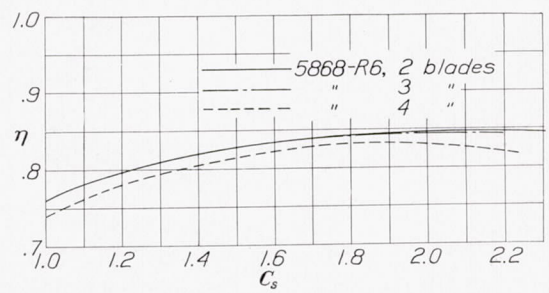

FIGURE 38.—Efficiency-curve envelopes for propellers having 2, 3, and 4 blades of R. A. F. 6 section.

sults. The curves do show, in spite of these minor inconsistencies, that the difference in peak efficiency between 2-blade, 3-blade, and 4-blade propellers is small.

The envelopes of the efficiency curves plotted against V/nD, as in figure 39, seem to bear out the theory that the difference in peak efficiencies of 2-blade, 3-blade,

and 4-blade propellers should grow less at higher values of blade angle. The opposite appears to be true, however, when, on a more practical basis, the efficiency-curve envelope is plotted against C_s, as in figure 37.

Figure 40 shows efficiency-curve envelopes for 2-blade and 3-blade propellers having the same solidity. The separation of the two curves is about 2 percent in this case. It should be pointed out, in connection with the results indicated in figures 36 and 40, that the blade thickness of the wide propeller was increased in proportion to its breadth (to maintain a constant thickness ratio and airfoil section) so that it is probably somewhat thicker than necessary for strength purposes. Part of the difference in the efficiency between the

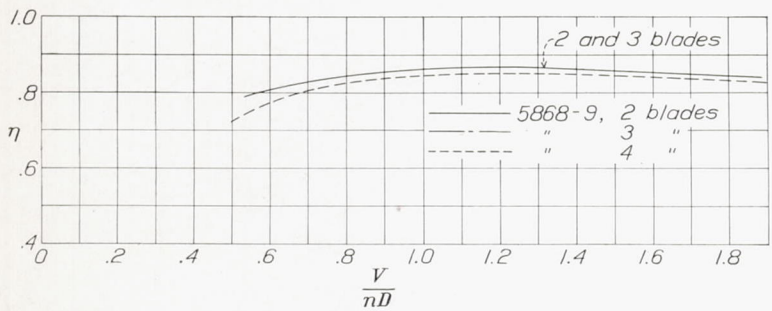

FIGURE 39.—Efficiency-curve envelopes (against V/nD) for propellers having 2, 3, and 4 blades of Clark Y section.

FIGURE 40.—Efficiency-curve envelopes for two propellers having the same solidity but a different number of blades.

2-blade and the 3-blade propellers having the same solidity would undoubtedly be offset by thinning the 2-blade propeller, although such a procedure would, of course, change the airfoil section.

A general comparison of the take-off qualities of the various propellers was not attempted as there was no basis of comparison that would have been entirely fair

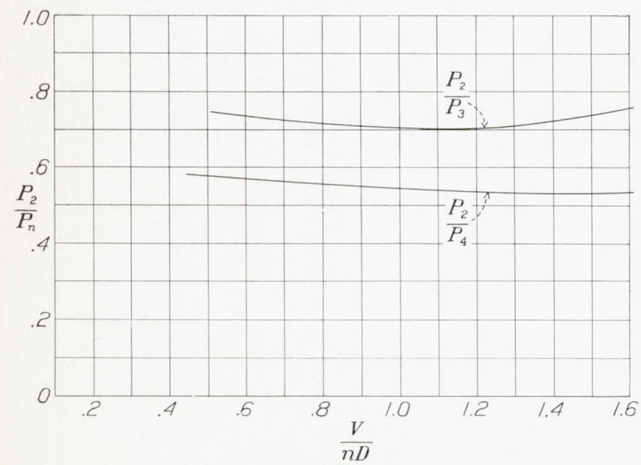

FIGURE 41.—Ratios of power absorbed by propellers having 2, 3, and 4 blades for the high-speed design condition.

to all propellers. Any designer having a choice of two or more propellers can calculate their thrusts in the take-off range by the methods given in the appendix of this report. The designer knowing the design limitations peculiar to his particular problem will thus be able to make a satisfactory comparison.

The lack of data for the 3-blade propeller in the past has resulted in the use of empirical methods of making 3-blade and 4-blade popeller selections from 2-blade-propeller data. As the propeller with the greater number of blades absorbs more power, it is customary to use a certain fraction of the available power in computing the value of C_s to be used with the 2-blade-propeller charts. This method is an approximation and will not give the optimum propeller diameter and blade angle for the design condition, although the difference may not be large. The convenience of this approximation has more than offset its faults and, now that data for 3-blade and 4-blade propellers are available, it is interesting to compare the ratios of the power absorbed by the 2-blade, 3-blade, and 4-blade propellers. Such a comparison is shown in figure 41; in figure 42 is shown a similar comparison for the 2-blade and 3-blade propellers having the same solidity. The curves in figure 41 represent the mean of the curves for the Clark Y and R. A. F. 6 propellers, which were separated by a small amount.

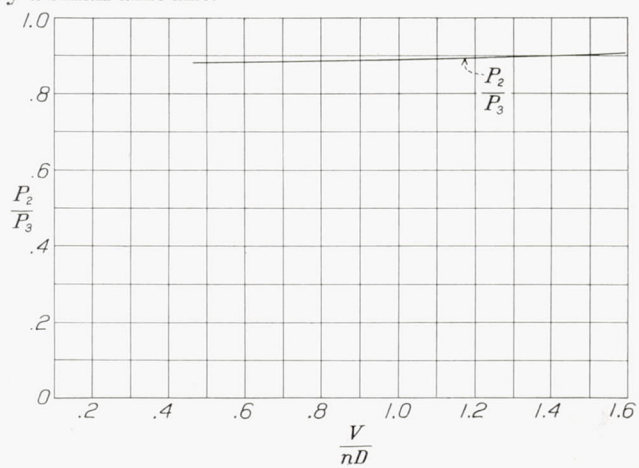

FIGURE 42.—Ratio of power absorbed by 2-blade and 3-blade propellers having the same solidity for the high-speed design condition.

Throughout the V/nD range shown in figure 41, the 2-blade propeller absorbs from 70 to 75 percent of the power absorbed by the 3-blade propeller and from 53 to 58 percent of the power absorbed by the 4-blade propeller. The 3-blade propeller 5868–R6 absorbs more power than the 2-blade propeller 37–3647, which has the same solidity. The ratio of their powers, P_2/P_3, varies (fig. 42) from 0.88 to 0.91.

The information given in figures 41 and 42 indicates that the power absorbed by two propellers having similar blades but different total blade areas is not directly proportional to the blade area; a direct relation may be used, however, when the differences in blade areas are small.

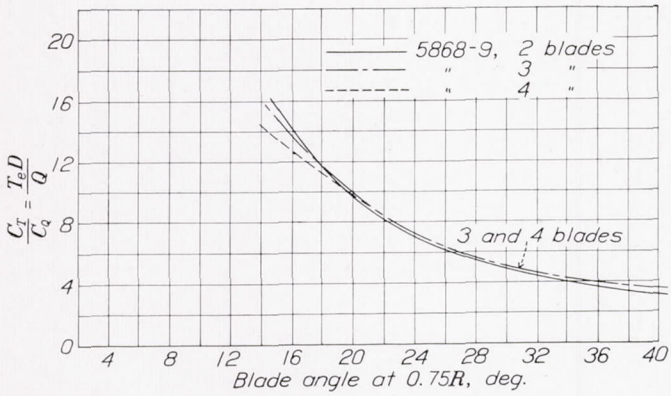

FIGURE 43.—Comparison of static-thrust characteristics of propellers having 2, 3, and 4 blades of Clark Y section.

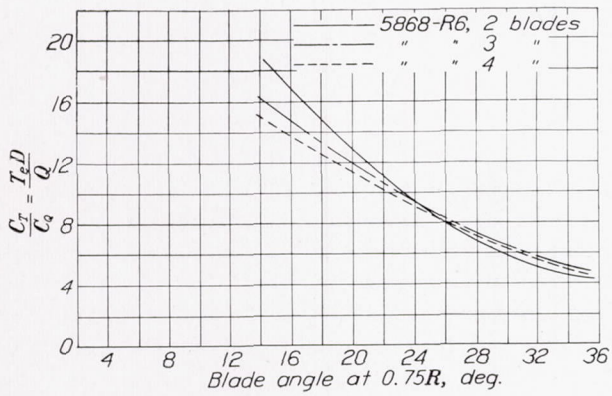

FIGURE 44.—Comparison of static-thrust characteristics of propellers having 2, 3, and 4 blades of R. A. F. 6 section.

Some interest has been shown in the past concerning the static thrust of propellers. Although static thrust has little importance in connection with the take-off problem, it may possibly be of interest for other reasons. Figures 43 and 44 have therefore been included; they are plots of C_T/C_Q, taken at $V/nD=0$, against blade angle for 2-blade, 3-blade, and 4-blade Clark Y and R. A. F. 6 propellers, respectively. As C_T/C_Q equals T_eD/Q, the curves represent the effective static thrust for any given value of torque and diameter. It is seen that, at blade angles above 20°, the static thrusts of the 3-blade and 4-blade propellers are higher than those for the 2-blade propeller. This result is due to the more favorable stalling characteristics of propellers of higher solidity.

CONCLUSIONS

1. The tests showed a 3-blade propeller to have a higher peak efficiency than a 2-blade propeller having the same solidity, thickness ratio, airfoil section, and diameter.

2. The loss in efficiency commonly conceived to be the result of increasing the solidity by adding blades was not fully realized. The tests showed only about 2 percent difference in peak efficiency between propellers having 2 and 4 blades.

3. An increase in solidity tended to delay the stall and to increase the efficiency in the take-off range.

LANGLEY MEMORIAL AERONAUTICAL LABORATORY,
NATIONAL ADVISORY COMMITTEE FOR AERONAUTICS,
LANGLEY FIELD, VA., *November 9, 1937.*

APPENDIX

SELECTION OF PROPELLERS AND THRUST CALCULATION

SELECTION

The type of C_s chart given in figures 7, 10, 14, 17, 24, 28, and 30 has been the standard N. A. C. A. design chart since 1929 (see reference 5) and its use requires but little explanation. In the selection of a propeller for any given engine and airplane, the first step is to calculate C_s from the equation:

$$C_s=\frac{0.638\times\text{m. p. h.}\times\left(\frac{\rho}{\rho_0}\right)^{\frac{1}{5}}}{(\text{b. hp.})^{\frac{1}{5}}\times(\text{r. p. m.})^{\frac{2}{5}}}$$

where the speed, the horsepower, and the engine revolution speed are the values representing the design conditions and ρ/ρ_0 is the relative density. With this value of C_s, project upward on the C_s chart to the broken line of maximum efficiency for C_s. This point determines the blade angle and a horizontal projection to the V/nD scale gives the design V/nD with which the diameter D may be calculated from the relation

$$D=\frac{\text{m. p. h.}\times 88}{\text{r. p. m.}\times\frac{V}{nD}}$$

The design efficiency is obtained by projecting upward from the design C_s to the envelope of the efficiency curves.

CALCULATION OF PROPELLER THRUST

The problem of calculating the thrust of a propeller throughout the take-off and the flight range of air speeds resolves itself into two parts, one for the controllable constant-speed propeller and the other for the fixed-pitch propeller.

Many varieties of specialized charts have been designed for such calculations, but the basic charts of C_T and C_P plotted against V/nD are the only ones actually necessary. The calculations are somewhat facilitated if lines of constant C_T are superimposed on the C_P chart, in which case only that one chart is necessary.

Constant-speed propeller.—The first step in calculating the take-off thrust for a particular airplane and propeller is to compute the value of the power coefficient C_P from the equation $C_P=P/\rho n^3D^5$. This equation may be put in the more usable form:

$$C_P=\frac{\text{b. hp.}}{2\,\frac{\rho}{\rho_0}\left(\frac{\text{r. p. m.}}{100}\right)^3\left(\frac{D}{10}\right)^5}$$

where b. hp. and r. p. m. are the take-off brake horsepower and engine speed and ρ/ρ_0 is the relative density of the air. For a constant-speed propeller, this value of C_P will remain constant throughout the take-off range and so may be represented by a straight line on the chart of C_P against V/nD. Now at even values of V/nD, pick off interpolated values of C_T along this straight line and compute $\eta=C_T/C_P\times V/nD$. Since the engine speed and diameter are constant, each value of V/nD represents a certain air speed, which may be obtained from the following relation:

$$V=\frac{\text{r. p. m.}\times D}{88}\times\frac{V}{nD}$$

in miles per hour. The propeller thrust is obtained from the relation

$$T=\frac{\text{b. hp.}\times\eta\times 375}{\text{m. p. h.}}=\text{constant}\times C_T$$

The foregoing simple method provides data for a plot of thrust against air speed for the take-off range of air speeds. The same method may be used for the climbing and flight range.

An obvious simplification would have been obtained if lines of constant efficiency instead of constant thrust coefficient had been superimposed on the C_P curves. Past experience, however, has shown that more accurate values of thrust may be obtained with the method here presented.

Fixed-pitch propellers.—It is assumed, in the use of the method of calculating the thrust for fixed-pitch propellers, that the following sea-level design characteristics of the airplane, the engine, and the propeller are known:

V_0, design air speed, m. p. h.

N_0, design engine speed, r. p. m.

$(\text{b. hp.})_0$, design engine power (rated power).

$\left(\frac{V}{nD}\right)_0=J_0$, design V/nD.

η_0, design efficiency (high speed or cruising).

D, propeller diameter, ft.

β_0, design blade angle at $0.75R$.

The method may conveniently be put into step form as follows:

1. Using J_0 and β_0, obtain C_{T_0} and C_{P_0} from charts of C_T and C_P against V/nD.

2. At even values of J pick off values of C_T and C_P along line of constant β_0 (interpolate when necessary).

3. Compute $\frac{J}{J_0}$, $\frac{C_T}{C_P}$, $\frac{C_{P_0}}{C_P}$

4. Compute $\frac{N}{N_0}=\sqrt{\frac{C_{P_0}}{C_P}}$

5. Compute $T_0=[\eta_0\times(\text{b. hp.})_0\times 375]/V_0$

6. Compute $V=V_0\times\frac{J}{J_0}\times\frac{N}{N_0}$

7. Compute thrust, $T=T_0\times\frac{C_{P_0}}{C_{T_0}}\times\frac{C_T}{C_P}=K\times\frac{C_T}{C_P}$

$$\text{where } K=\frac{T_0C_{P_0}}{C_{T_0}}$$

This method assumes that the full-throttle engine torque is constant.

As an example, assume that it is desired to obtain the propeller thrust through the take-off and climbing ranges for an airplane having the following characteristics:

$V_0=190$; $N_0=1{,}500$; $(\text{b.hp.})_0=600$; $J_0=1.00$; D_0(2-blade)=11 feet 1½ inches; $\eta_0=0.862$; $\beta_0=25°$.

Blade section=Clark Y.

The computed data may be conveniently tabulated as follows:

$C_{T_0}=0.0448$; $C_{P_0}=0.0520$; $T_0=1{,}020$ lb.; $J_0=1.00$.

J	J/J_0	C_T	C_P	C_T/C_P	C_{P_0}/C_P	N/N_0	V (m. p. h.)	T (lb.)
0.1	0.1	0.110	0.1056	1.042	0.493	0.702	13.3	1,232
.2	.2	.1075	.1017	1.059	.512	.720	27.4	1,252
.3	.3	.1058	.0972	1.088	.535	.731	41.7	1,287
.4	.4	.1055	.0911	1.158	.571	.755	57.4	1,370
.5	.5	.1037	.0858	1.207	.607	.778	74.0	1,427
.6	.6	.0970	.0823	1.178	.632	.795	90.6	1,392
.7	.7	.0870	.0790	1.100	.658	.811	108.0	1,300
.8	.8	.0748	.0732	1.022	.710	.842	128.0	1,210

$$K=\frac{0.0520}{0.0448}\times 1{,}020=1{,}182$$

Effect of blade width and body.—The two methods given of calculating thrust, and also the method of selecting propellers, assumed that the propellers under consideration had the same blade width as the ones for which the data are given in this report. Frequently it may be required to find the diameter, the design blade-angle setting, and the thrust of a propeller having a blade width slightly different from those tested. As was mentioned earlier, it may be assumed that the power and the thrust vary directly with the blade areas (or blade widths) for propellers with similar shape characteristics where the differences in areas are small.

In the calculation of C_s, the power should therefore be multiplied by the ratio of the blade widths b_1/b_2, where b_1 is the blade width at three-quarters radius of the propeller for which the design charts were made and b_2 is the blade width at the same radius for the propeller under consideration.

The same ratio should be used in calculating the value of C_P to be used in obtaining the take-off thrust, and the take-off thrust obtained from the charts should be divided by this ratio to obtain the actual thrust of the propeller.

Similarly, corrections are necessary in the case where the body under consideration is greatly different from the liquid-cooled engine nacelle with which the present tests were made. Some information with regard to the effect of the body on the propulsive efficiency may be obtained from reference 2. The added drag of those parts of the airplane in the slipstream (other than the body itself) should also be considered. Parts of the wing, the tail surfaces, and the landing gear are often in the propeller slipstream and their added drag due to the slipstream may be approximated from the following relation:

$$\frac{\Delta D}{D}=2.5C_T/J^2$$

where ΔD is the added drag and D is the drag without slipstream.

The test data for a propeller having one airfoil section should not be used to calculate the performance of a propeller having another airfoil section.

It is shown in reference 3 that compressibility often has a marked effect on the performance of a propeller in the take-off range. The necessary corrections for compressibility are not easily applied but methods of making such corrections are explained in reference 3.

REFERENCES

1. Weick, Fred E., and Wood, Donald H.: The Twenty-Foot Propeller Research Tunnel of the National Advisory Committee for Aeronautics. T. R. No. 300, N. A. C. A., 1928.
2. Biermann, David, and Hartman, Edwin P.: Tests of Five Full-Scale Propellers in the Presence of a Radial and a Liquid-Cooled Engine Nacelle, Including Tests of Two Spinners. T. R. No. 642. N. A. C. A., 1938.
3. Biermann, David, and Hartman, Edwin P.: The Effect of Compressibility of Eight Full-Scale Propellers Operating in the Take-Off and Climbing Range. T. R. No. 639. N. A. C. A., 1938.
4. Glauert, H.: Airplane Propellers. Vol. IV, div. L of Aerodynamic Theory, W. F. Durand, ed., Julius Springer (Berlin), 1935, p. 261.
5. Weick, Fred E.: Working Charts for the Selection of Aluminum Alloy Propellers of a Standard Form to Operate with Various Aircraft Engines and Bodies. T. R. No. 350, N. A. C. A., 1930.

U. S. GOVERNMENT PRINTING OFFICE: 1938

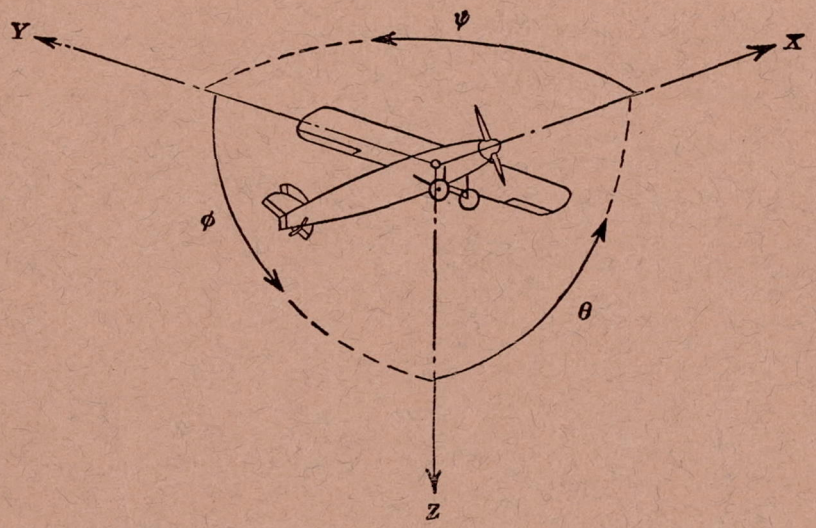

Positive directions of axes and angles (forces and moments) are shown by arrows

Axis		Force (parallel to axis) symbol	Moment about axis			Angle		Velocities	
Designation	Symbol		Designation	Symbol	Positive direction	Designation	Symbol	Linear (component along axis)	Angular
Longitudinal	X	X	Rolling	L	$Y \longrightarrow Z$	Roll	ϕ	u	p
Lateral	Y	Y	Pitching	M	$Z \longrightarrow X$	Pitch	θ	v	q
Normal	Z	Z	Yawing	N	$X \longrightarrow Y$	Yaw	ψ	w	r

Absolute coefficients of moment

$C_l = \frac{L}{qbS}$ (rolling) $\quad C_m = \frac{M}{qcS}$ (pitching) $\quad C_n = \frac{N}{qbS}$ (yawing)

Angle of set of control surface (relative to neutral position), δ. (Indicate surface by proper subscript.)

4. PROPELLER SYMBOLS

D, Diameter

p, Geometric pitch

p/D, Pitch ratio

V', Inflow velocity

V_s, Slipstream velocity

T, Thrust, absolute coefficient $C_T = \frac{T}{\rho n^2 D^4}$

Q, Torque, absolute coefficient $C_Q = \frac{Q}{\rho n^2 D^5}$

P, Power, absolute coefficient $C_P = \frac{P}{\rho n^3 D^5}$

C_s, Speed-power coefficient $= \sqrt[5]{\frac{\rho V^5}{P n^2}}$

η, Efficiency

n, Revolutions per second, r.p.s.

Φ, Effective helix angle $= \tan^{-1}\left(\frac{V}{2\pi r n}\right)$

5. NUMERICAL RELATIONS

1 hp.=76.04 kg-m/s=550 ft-lb./sec.
1 metric horsepower=1.0132 hp.
1 m.p.h.=0.4470 m.p.s.
1 m.p.s.=2.2369 m.p.h.

1 lb.=0.4536 kg.
1 kg=2.2046 lb.
1 mi.=1,609.35 m=5,280 ft.
1 m=3.2808 ft.